



Temperature sensitivity of dark CO₂ fixation in temperate forest soils

Rachael Akinyede^{1,2}, Martin Taubert¹, Marion Schrumpp², Susan Trumbore², and Kirsten Küsel^{1,3}

¹Aquatic Geomicrobiology, Institute of Biodiversity, Friedrich Schiller University Jena, Dornburger Str. 159, 07743 Jena, Germany

²Department of Biogeochemical Processes, Max Planck Institute for Biogeochemistry, Hans-Knöll Str. 10, 07745 Jena, Germany

³German Centre for Integrative Biodiversity Research (iDiv) Halle–Jena–Leipzig, Puschstraße 4, 04103 Leipzig, Germany

Correspondence: Kirsten Küsel (kirsten.kuesel@uni-jena.de)

Received: 1 April 2022 – Discussion started: 28 April 2022

Revised: 28 July 2022 – Accepted: 4 August 2022 – Published: 1 September 2022

Abstract. Globally, soil temperature to 1 m depth is predicted to be up to 4 °C warmer by the end of this century, with pronounced effects expected in temperate forest regions. Increased soil temperatures will potentially increase the release of carbon dioxide (CO₂) from temperate forest soils, resulting in important positive feedback on climate change. Dark CO₂ fixation by microbes can recycle some of the released soil CO₂, and CO₂ fixation rates are reported to increase under higher temperatures. However, research on the influence of temperature on dark CO₂ fixation rates, particularly in comparison to the temperature sensitivity of respiration in soils of temperate forest regions, is missing. To determine the temperature sensitivity (Q_{10}) of dark CO₂ fixation and respiration rates, we investigated soil profiles to 1 m depth from beech (deciduous) and spruce (coniferous) forest plots of the Hummelshain forest, Germany. We used ¹³C-CO₂ labelling and incubations of soils at 4 and 14 °C to determine CO₂ fixation and net soil respiration rates and derived the Q_{10} values for both processes with depth. The average Q_{10} for dark CO₂ fixation rates normalized to soil dry weight was 2.07 for beech and spruce profiles, and this was lower than the measured average Q_{10} of net soil respiration rates with ~ 2.98. Assuming these Q_{10} values, we extrapolated that net soil respiration might increase 1.16 times more than CO₂ fixation under a projected 4 °C warming. In the beech soil, a proportionally larger fraction of the label CO₂ was fixed into soil organic carbon than into microbial biomass compared to the spruce soil. This suggests a primarily higher rate of microbial residue formation (i.e. turnover as necromass or release

of extracellular products). Despite a similar abundance of the total bacterial community in the beech and spruce soils, the beech soil also had a lower abundance of autotrophs, implying a higher proportion of heterotrophs when compared to the spruce soil; hence this might partly explain the higher rate of microbial residue formation in the beech soil. Furthermore, higher temperatures in general lead to higher microbial residues formed in both soils. Our findings suggest that in temperate forest soils, CO₂ fixation might be less responsive to future warming than net soil respiration and could likely recycle less CO₂ respired from temperate forest soils in the future than it does now.

1 Introduction

Most of Earth's terrestrial carbon stock is found in soils, with ~ 36 % occurring in the top 1 m depth of forest soils (Jobbágy and Jackson, 2000) based on the new carbon inventory of the global soil carbon pool (Hugelius et al., 2014; Schuur et al., 2015). Decomposition of soil organic carbon (SOC) provides one of the largest sources of carbon dioxide (CO₂) to the atmosphere (Rastogi et al., 2002; Lal, 2004). Microbes can re-fix 3 %–6 % of CO₂ in temperate forest mineral soils before its release to the atmosphere (Akinyede et al., 2020; Spohn et al., 2019), through so-called dark CO₂ fixation (Miltner et al., 2005; Šantrůčková et al., 2018). Dark CO₂ fixation in soils is mediated by chemolithoautotrophic bacteria, largely via the Calvin–Benson–Bassham (CBB) path-

way (Niederberger et al., 2015; Wu et al., 2014), the Wood–Ljungdahl pathway (WLP), or the reverse tricarboxylic acid (rTCA) pathway (Beulig et al., 2016; Liu et al., 2018). Heterotrophic bacteria can also contribute to dark CO₂ fixation via anaerobic carboxylation reactions associated with central microbial metabolism (Erb, 2011). The genetic potential for both autotrophic and heterotrophic CO₂ fixation has been demonstrated in various soils (Miltner et al., 2005; Šantrůčková et al., 2018) including temperate forest soils (Akinyede et al., 2022a, 2020; Kaiser et al., 2016).

The biomass of microbial communities serves as the entry point of carbon fixed from CO₂ into SOC, which includes both the intact microbial biomass carbon (MBC) pool and released microbial residues (Miltner et al., 2004, 2005; Spohn et al., 2019). Microbial residues constitute any non-living organic material of microbial origin including necromass and extracellular metabolites (Geyer et al., 2020). Since the transformation of CO₂ and release of the fixed carbon via microbial residues vary for different microbial groups (Berg et al., 2011; Miltner et al., 2005), the composition and abundance of microbial communities play a vital role in CO₂ fixation rates in soils. High CO₂ fixation rates in soils have been reportedly associated with higher abundance of obligate autotrophs and specific bacterial groups like Proteobacteria (Long et al., 2015; Xiao et al., 2018). As the microbial communities fixing CO₂ are sensitive to changes in edaphic conditions (Berg, 2011; Hügler and Sievert, 2011), various biotic and abiotic predictors of CO₂ fixation rates have been identified. Factors like CO₂ concentration (Beulig et al., 2016; Spohn et al., 2019; Akinyede et al., 2020), SOC content and quality (Miltner et al., 2005; Šantrůčková et al., 2018; Xiao et al., 2018; Akinyede et al., 2022a), and pH (Šantrůčková et al., 2005; Long et al., 2015) affect dark CO₂ fixation rates in many soils including those of temperate forests.

Here, we focus on temperature as a factor determining soil CO₂ fixation rates. Biological processes are generally faster under higher temperatures due to accelerated rates of enzymatic reactions (Arrhenius, 1889; Van 't Hoff, 1898; Davidson and Janssens, 2006). Hence, temperature presumably affects dark CO₂ fixation rates but also the rates of CO₂ production through decomposition. If moisture is not limiting, warmer temperatures increase CO₂ emission from temperate forest soils (Melillo et al., 2017, 2011, 2002; Walker et al., 2018; Winkler et al., 1996), and the degree of response is similar to depths of 1 m (Hicks Pries et al., 2017; Soong et al., 2021). Such responses coincide with a reduction in the total SOC pool and have been mostly attributed to increased microbial respiration (Melillo et al., 2011). The net change in total CO₂ efflux from soil (net soil respiration) includes the effects of temperature on both CO₂ production (decomposition) and CO₂ fixation. These effects may change with soil depth from the relatively organic carbon-rich surface soils to the more carbon-limited deeper soils.

A previous study describing the influence of temperature on CO₂ fixation rates described ~ 10 times higher fixation

rates at 25 °C than at 4 °C in a range of mostly Alisol and Retisol soils in afro-temperate forest and grassland ecosystems of the lower-latitude regions (Nel and Cramer, 2019), suggesting potentially large temperature effects on CO₂ fixation rates. However, a systematic study comparing the responses of dark CO₂ fixation and net soil respiration from temperate forest soils is currently lacking. The relative temperature responses of these processes are important because globally, soil temperatures are projected to warm by ~ 4 °C until 2100 (based on simulations under the Representative Concentration Pathway (RCP) 8.5 scenario; IPCC, 2013; Soong et al., 2020).

The temperature sensitivity (Q_{10}), the increase in reaction rates for a 10 °C rise in temperature, is a commonly reported value when describing the response of soil microbial processes to higher temperatures (Davidson and Janssens, 2006; Fang et al., 2005; Leifeld and Fuhrer, 2005). Hicks Pries et al. (2017) reported a Q_{10} of 2.4 for net respiration rates in temperate coniferous forest soil. Similar Q_{10} values of between 2 and 3 for net respiration rates have also been described for other soil environments (Conant et al., 2008; Li et al., 2021). Considering that dark CO₂ fixation rates and soil respiration rates increase with temperature as described above and that dark CO₂ fixation rates have been shown to correlate linearly with net soil respiration rates (Miltner et al., 2005; Šantrůčková et al., 2018), the Q_{10} values of dark CO₂ fixation rates with depth might correlate with those of net soil respiration rates.

This study describes the temperature sensitivity (Q_{10}) of dark CO₂ fixation rates and compares it to that of net soil respiration rates across soil profiles of deciduous and coniferous forests, the two temperate forests based on vegetation (Dreiss and Volin, 2014; Adams et al., 2019). Soils of two acidic forest plots from the Hummelshain forest, Germany, dominated by beech (deciduous) and spruce (coniferous) tree species were incubated under two temperature conditions (4 and 14 °C). We used a ¹³CO₂-labelling approach to quantify dark CO₂ fixation rates. We also measured net soil respiration rates and determined the Q_{10} values of both processes across depth. We thus hypothesize that the Q_{10} values of dark CO₂ fixation rates with depth correlate with those of net soil respiration rates. Using the derived Q_{10} values, we evaluated the potential changes in dark CO₂ fixation rates and net soil respiration rates under projected increase in global soil temperature. We further explored the microbial community composition in the beech and spruce soil, with the aim to assess potential differences in the community that might influence dark CO₂ fixation rates and, thereby, its Q_{10} across temperate forest soil profiles.

2 Materials and methods

2.1 Site description and soil classification

The study sites (beech plot 50°45′28.0″ N, 11°37′21.0″ E; spruce plot 50°45′30.0″ N, 11°37′23.0″ E) are located within the forested areas of the Hummelshain municipality (~362 m a.s.l.) in Thuringia, central Germany. The study site was established on a former coniferous forest, and it involved the planting of European beech trees within Norway spruce and Scot's pine stands. The main purpose for this conversion was to counteract the low pH of the topsoil under the coniferous stands and, thus, biologically activate the forest floors (Graser, 1928). The mean annual rainfall in this area is about 630 mm, and the mean annual air temperature is around 7.8 °C (Achilles et al., 2020). The two study plots located < 1 km apart are dominated by European beech (*Fagus sylvatica* L.) and Norway spruce (*Picea abies* (L.) H.Karst.) tree stands, respectively, and feature similar soil geology (Achilles et al., 2020). The soils are mostly sandy (40%–50% sand and silt) with a clay enrichment with depth (Table 1; Eckelmann et al., 2006; Bormann, 2007) due to the Triassic sandstone bedrock in the Hummelshain area (Achilles et al., 2020). The soils in this region are predominantly quartz-rich (50%–60% quartz), consisting of sandstones and silt–mud stones, and are classified as Luvisols with an F-mull-over-loess layer (IUSS Working Group WRB, 2015; Achilles et al., 2020). Both soils feature a low pH (< 4) and a high C/N ratio (Table 1). The beech soil was slightly lower in SOC, MBC, total nitrogen (TN), and moisture content than the spruce soil across depth. The beech soil profile also featured a lower clay but higher sandy texture when compared to the spruce soil profile. Further description of the forest sites and the soil characteristics in the Hummelshain locality can be found in Achilles et al. (2020).

2.2 Sampling design

The sampling was carried out in September 2020, towards the end of the summer season. By driving in an 84 mm wide closed auger into the soil with the aid of a motor hammer (Cobra Combi, Atlas Copco AB, Nacka, Sweden), 6 replicate soil cores, 1–2 m apart, were obtained from each of the sampling plots, leading to a total of 12 soil cores for the beech and spruce plots. To avoid direct impact from stem flow and to prevent larger roots from impeding the soil coring process, all soil cores were taken ~2 m away from the base of the trees. Soil sampling began from the mineral horizon, and the organic layer was ignored. Three segments were extracted from each soil core by depths chosen according to the similarity of the horizon among all replicate cores to obtain samples representing the AB horizon (0–20 cm), Bv horizon (20–55 cm), and BvT horizon (55–100 cm) for the beech plot and the AB horizon (0–20 cm), Bv horizon (20–55 cm), and BvT horizon (55–92 cm) for the spruce sample plot. Soil sam-

ples from the same depth intervals of each of the six replicate cores were homogenized in pairs to yield three replicate cores each for the beech and spruce forest plot. Afterwards, all soil samples were sieved using a 2 mm sieve to remove stones and roots prior to the incubation experiments. Fresh subsamples for later DNA extraction and geochemical analysis were also taken and immediately stored by freezing in liquid nitrogen.

2.3 Geochemical parameters and isotope measurements

The total and inorganic carbon and nitrogen concentration, pH, and gravimetric water content as well as carbon isotope signatures of all soil samples were determined as previously described by Akinyede et al. (2020) with values reported in Tables 1 and S1 in the Supplement. The ¹³C signature of the bulk soil total organic carbon was analysed using an elemental analyser isotope ratio mass spectrometer (EA-IRMS) (EA 1110, CE Instruments, Milan, Italy) coupled to a Delta⁺ IRMS (Thermo Finnigan, Bremen, Germany) through a ConFlo III interface. The extraction of microbial biomass carbon content was performed by chloroform fumigation extraction (CFE) (Nowak et al., 2015; Vance et al., 1987) using 0.05 M K₂SO₄ following methods described previously (Akinyede et al., 2020). The microbial biomass carbon content (MBC) extracted as the chloroform soluble carbon content was derived by taking the difference between the dissolved organic carbon (DOC) content in the unfumigated (C_{unfum}) and the fumigated soil extract fractions (C_{fum}) for all soil samples. Values from all samples were divided by a correction factor K_{EC} (of 0.45) that accounts for the extraction efficiency. This factor corrects for the incomplete release of carbon from the living microbial cells into the solution and is widely applied to different soils (Joergensen and Mueller, 1996; Joergensen et al., 2011; Wu et al., 1990) as CFE only measures the fraction of microbial biomass rendered extractable in K₂SO₄ solution after lysis with chloroform, which is likely the very labile microbial fraction (e.g. the cytoplasm) (Ocio and Brookes, 1990; Wu et al., 1990). The MBC content was thus calculated as follows:

$$\text{MBC (mg)} = \frac{[C_{\text{fum}} - C_{\text{unfum}}]}{K_{\text{EC}}}. \quad (1)$$

Despite previous studies showing no strong variations in the K_{EC} of 0.45 between soils or incubation temperatures (Martens, 1995; Joergensen et al., 2011), we cannot exclude possible effects resulting from differences in CFE efficiency on our results, especially in comparisons of the rates across the different soil depths or between the beech and spruce soils.

To determine the δ¹³C signature of the bulk soil MBC, the ¹³C signature of the DOC from the fumigated and unfumigated CFE fractions was analysed using an isotope ratio mass spectrometer (DELTA V IRMS, Thermo Fisher Scien-

Table 1. Geochemical properties of soil cores obtained from beech and spruce soil plots at the Hummelshain forest. Soil pH, moisture content, soil organic carbon (SOC), carbon / nitrogen (C/N) ratio, microbial biomass carbon (MBC), total nitrogen (TN), MBC / SOC ratio, natural abundance of ¹³C of SOC and MBC, bacterial abundance (*16S rRNA* gene copies), and soil texture class are reported for three depths definitions for the beech and spruce soils of the Hummelshain forest. Each reported value represents the mean of three replicate soil cores taken from bulk soils during the sampling campaign. The abbreviation “dw” denotes dry weight.

	Depth – horizon (cm)					
	Beech			Spruce		
	AB (0–20)	Bv (20–55)	BvT (55–100)	AB (0–20)	Bv (20–55)	BvT (55–100)
pH	3.32 ± 0.08	3.47 ± 0.03	3.13 ± 0.03	2.84 ± 0.03	3.16 ± 0.02	3.07 ± 0.06
Moisture (%)	8.65 ± 1.30	8.28 ± 0.84	11.27 ± 1.41	10.34 ± 2.22	10.95 ± 0.66	14.27 ± 1.07
SOC (%)	0.90 ± 0.12	0.28 ± 0.11	0.12 ± 0.03	1.56 ± 0.07	0.33 ± 0.13	0.21 ± 0.05
C/N ratio	20.42 ± 1.77	11.23 ± 3.02	5.59 ± 0.83	19.13 ± 1.02	9.97 ± 2.37	6.38 ± 1.02
MBC (μg C g ⁻¹ (dw))	74.14 ± 3.08	21.92 ± 6.53	14.26 ± 6.30	84.83 ± 9.42	25.39 ± 12.85	19.43 ± 6.71
TN (%)	0.04 ± 0.004	0.02 ± 0.002	0.02 ± 0.002	0.08 ± 0.005	0.03 ± 0.005	0.03 ± 0.002
MBC/SOC (%)	0.84 ± 0.15	0.80 ± 0.09	1.05 ± 0.34	0.55 ± 0.08	0.74 ± 0.10	0.96 ± 0.07
δ ¹³ C-SOC (‰)	-27.14 ± 0.41	-25.96 ± 0.16	-25.37 ± 0.27	-27.62 ± 0.16	-25.53 ± 0.31	-25.25 ± 0.14
δ ¹³ C-MBC (‰)	-23.62 ± 0.97	-22.45 ± 0.59	-22.71 ± 0.22	-21.57 ± 0.64	-22.05 ± 0.85	-22.67 ± 0.66
<i>16S rRNA</i> (copies g ⁻¹ (dw))	1.83 × 10 ⁹ ± 8.18 × 10 ⁸	7.0 × 10 ⁸ ± 2.37 × 10 ⁸	1.19 × 10 ⁸ ± 1.06 × 10 ⁸	2.40 × 10 ⁹ ± 3.68 × 10 ⁸	5.47 × 10 ⁸ ± 2.67 × 10 ⁸	3.89 × 10 ⁸ ± 2.22 × 10 ⁸
Soil texture class (Eckelmann et al., 2006; Bormann, 2007)	Highly silty sand (Su4)	Loamy silty sand (Slu)	Slightly clay loam (Lt2)	Loamy sandy silt (Uls)	Medium clayey silt (Ut3)	Loamy clay (Tl)

tific, Bremen, Germany) coupled to a high-performance liquid chromatography (HPLC) system (UltiMate 3000, Dionex Softron GmbH, Germering, Germany) via an LC IsoLink interface (Thermo Fisher Scientific, Bremen, Germany). All ¹³C isotope ratios were reported in the delta notation (δ) expressed as δ¹³C values (¹³C/¹²C ratios) in per mil (‰), relative to the international reference material Vienna Pee Dee Belemnite (V-PDB) (Coplen et al., 2006).

$$\delta^{13}\text{C} (\text{‰}) = \left[\frac{\frac{^{13}\text{C}}{^{12}\text{C}} \text{ sample}}{\frac{^{13}\text{C}}{^{12}\text{C}} \text{ reference}} - 1 \right] \times 1000 \quad (2)$$

Afterwards, the δ¹³C in per mil (‰) of microbial biomass carbon (MBC) was derived by applying an isotope mass balance to the measured ¹³C signals measured for all fumigated and unfumigated DOC fractions from CFE as previously described (Akinyede et al., 2020).

$$\delta^{13}\text{C}_{\text{MB}} (\text{‰}) = \frac{[\delta^{13}\text{C}_{\text{fum}} \times C_{\text{fum}} - \delta^{13}\text{C}_{\text{unfum}} \times C_{\text{unfum}}]}{C_{\text{fum}} - C_{\text{unfum}}} \quad (3)$$

2.4 ¹³C-CO₂-labelling incubation experiment

The CO₂ fixation rates were determined using microcosm incubations. Four replicates for each sieved soil sample (60 g wet weight) obtained from all six soil cores in both the

beech and the spruce sampling plots were placed in sterilized 1000 mL serum bottles, closed with butyl rubber stoppers. The large headspace-to-soil-volume ratio was chosen to ensure minimal changes in the headspace CO₂ concentration and the ¹³C isotope signatures as no further additions to the headspace CO₂ were performed throughout the incubation period with labelled ¹³CO₂. The four replicate jars were split into two pairs of two replicates each prior to a 4 d preincubation period. The first pair was preincubated at 4 °C and the second at 14 °C. Before preincubation, all jars were opened for several minutes to allow the CO₂ concentration in the jar to equilibrate with the ambient concentration. After the preincubation period, gas samples were obtained with the aid of a gas syringe for CO₂ measurement. Afterwards, the jars were opened, and homogenized soil samples were subsampled for (1) the determination of total and organic carbon and nitrogen content as well as ¹³C isotope signatures of the bulk soil, (2) extraction to determine initial microbial biomass carbon content and its ¹³C isotope signature, and (3) storage for later DNA analysis.

The remainder of the soil (~ 30 g) was placed in the incubation jar, which was then flushed with synthetic air (75 % N₂ and 25 % O₂). One replicate of each temperature set was adjusted to 2 % (v/v) ¹³C-CO₂ in the headspace, and the second replicate was adjusted to 2 % (v/v) headspace ¹²C-CO₂ concentration, serving as treatments and controls, respectively. All soils exposed to the 2 % (v/v) ¹³C-CO₂, and con-

trols were then incubated statically in the dark for 21 d under the same temperature as used in the preincubation phase (4 and 14 °C). At the end of the incubation period, microcosms were opened and soil samples from all incubations were split into three parts, and geochemical parameters were analysed as after the preincubation phase. Parameters like SOC, MBC, the C/N ratio, and water content measured after incubation for the beech and spruce plots are described in Table S2 in the Supplement and did not differ with temperature and throughout the incubation period. In addition, the $\delta^{13}\text{C}$ signals of MBC and SOC from all incubated soil samples were measured as done for the bulk soil prior to the start of the rate measurements.

2.5 Determination of CO₂ fixation rates, respiration rates, and temperature sensitivity (Q_{10})

To calculate the CO₂ fixation rates for all soil incubations at both 4 and 14 °C, the actual $^{13}\text{C}/^{12}\text{C}$ ratio taken up into the total soil pool and into microbial biomass carbon (MBC) pool was measured as described in Sect. 2.3. This was derived from the measured and derived ^{13}C values (for all treatments (^{13}C labelled) and controls (^{13}C unlabelled/natural abundance)) of SOC and MBC, respectively.

The $^{13}\text{C}/^{12}\text{C}$ ratios were calculated based on the $^{13}\text{C}/^{12}\text{C}$ ratio of the international V-PDB standard as done previously (Akinyede et al., 2020, 2022a), where 0.0111802 is taken as the $^{13}\text{C}/^{12}\text{C}$ ratio of the international V-PDB standard (Werner and Brand, 2001):

$$\frac{^{13}\text{C}}{^{12}\text{C}} = \left[\frac{\delta^{13}\text{C}}{1000} + 1 \right] \times 0.0111802. \quad (4)$$

Subsequently, the excess ^{13}C ratio for the soil pool and the MBC pool was derived from the increase in the $^{13}\text{C}/^{12}\text{C}$ ratio between the ^{13}C -labelled treatment and the ^{12}C -labelled controls (^{13}C natural abundance level) normalized to the respective carbon content of the soil and of the microbial biomass (MBC) as follows:

$$\text{excess } ^{13}\text{C} \text{ (mg)} = \frac{^{13}\text{C}_{\text{labelled}}}{^{12}\text{C}_{\text{labelled}}} \times \text{MBC/SOC} - \frac{^{13}\text{C}_{\text{unlabelled}}}{^{12}\text{C}_{\text{unlabelled}}} \times \text{MBC/SOC}. \quad (5)$$

These values were then divided by the incubation time and expressed per gram of the bulk soil dry weight and per gram of microbial biomass carbon to obtain the CO₂ fixation rates per gram of soil dry weight ($\text{g}^{-1} \text{ (dw) soil d}^{-1}$) and per gram of MBC ($\text{g}^{-1} \text{ MBC d}^{-1}$), respectively.

Following Spohn et al. (2019), the net respiration rates for all soil preincubations were determined based on the difference in the CO₂ concentrations of the glass jars measured at the beginning and at the end of the incubation period using a gas chromatograph system for trace gas analysis of air samples (Agilent 6890 GC FID ECD PDD, USA). Gas samples

were taken from the headspace of the jars using a gas syringe attached to 250 mL evacuated vials. A period of 30 s was allowed for the gas vials to equilibrate with the incubation jars, after which the gas vials were disconnected from the vials and connected via a gas line to the gas chromatograph system for CO₂ measurement (in ppm). Using the ideal gas equation, net soil respiration rates were calculated according to Dossa et al. (2015), expressed as micrograms of carbon per gram of soil dry weight per day. As net respiration rates represent CO₂ produced minus CO₂ fixed, the total CO₂ production or decomposition rates were subsequently derived by adding the net respiration rates to the CO₂ fixation rates measured for all beech and spruce soil samples.

The temperature sensitivities of the CO₂ fixation (per unit soil and MBC) and net respiration rates (per gram of soil only), as well as the decomposition rate (per gram of soil only), were determined by calculating Q_{10} values according to Leifeld and Fuhrer (2005):

$$Q_{10} = \left[\frac{k_2}{k_1} \right]^{\left(\frac{10}{T_2 - T_1} \right)}, \quad (6)$$

where T_2 and T_1 denote the higher and lower temperatures (in °C) at which the soils were incubated, and k_2 and k_1 represent the corresponding derived CO₂ fixation rates, net respiration rate and decomposition rates for temperatures T_2 and T_1 , respectively.

2.6 DNA extraction and 16S rRNA gene sequencing

DNA was extracted from 0.25 g of all bulk soil and incubation samples using the DNeasy PowerSoil DNA kit (Qiagen, Hilden, Germany) according to the manufacturer's protocol. For Illumina MiSeq sequencing, libraries of amplicon sequences of bacterial 16S rRNA genes were generated. All libraries were prepared with the NEBNext Ultra DNA Library Prep Kit for Illumina (New England Biolabs, Hitchin, UK) using a two-step barcoding approach. For the first step, forward (Bact_341F) and reverse (Bact_785R) primers targeting the V3 to V4 hypervariable regions of the bacterial 16S rRNA gene were used (Klindworth et al., 2013). For Illumina sequencing, the primers were modified with an adaptor overhang which allowed for barcoding in a second PCR step. During the first PCR step, all DNA samples ($> 10 \text{ ng } \mu\text{L}^{-1}$) were amplified in a 20 μL reaction volume containing 10 μM of each primer, 0.67 $\mu\text{g } \mu\text{L}^{-1}$ of BSA (bovine serum albumin), 5.67 μL nuclease-free water, and 10 μL HotStarTaq Master Mix (Qiagen, Hilden, Germany). The PCR conditions used consisted of an initial denaturation at 95 °C for 45 min, followed by 26 to 30 cycles of denaturation (94 °C for 45 s), annealing (55 °C for 45 s), and extension (72 °C for 45 s) and then a final extension step at 72 °C for 10 min. While samples from the AB and Bv horizon were amplified using 26 to 27 cycles, a few samples from the BvT depth with low DNA concentration were amplified using 30 cycles with the same

cycling conditions. All amplified sequences from the first PCR step were barcoded in a second PCR step using 1 µL of the initial PCR products, 0.5 µM of barcoded primer set from Illumina (sequences provided in Table S4 in the Supplement), and Ruby Taq Master Mix (Jena Bioscience, Germany) following the cycling conditions of 6 cycles at 95 °C for 45 s, 55 °C for 45 s, and 72 °C for 45 s for denaturing, annealing, and extension steps, respectively. All samples were analysed by gel electrophoresis using 1 % agarose gel to ensure all amplicons were ~ 500 bp in length. Subsequently, prepared libraries were sequenced on a MiSeq (Illumina, Inc, San Diego, CA, USA) using v3 chemistry (2 × 250 bp).

The raw sequences generated were analysed using mothur (Schloss et al., 2009; <http://www.mothur.org>, last access: 19 January 2021) and the mothur MiSeq SOP as of 19 January 2021. Paired reads were combined, and sequences were trimmed, saving only sequences with the desired length of between 360 and 500 bp. Trimmed sequences were aligned to the SILVA reference database v132 release (Quast et al., 2013), and sequences with differences of up to four bases were pre-clustered. Chimeras were removed using UCHIME and the GOLD reference database implemented in mothur (Edgar et al., 2011). Subsequently, the taxonomic classification of the sequences against the SILVA database was performed.

2.7 Determination of chemolithoautotrophic CO₂ fixation potential in the Hummelshain forest soils

To determine the potential for chemolithoautotrophic CO₂ fixation among all soil samples, the abundance of functional genes involved in autotrophic CO₂ fixation was first predicted for all bacteria communities. Here, the representative sequences from operational taxonomic unit (OTUs) generated from mothur were analysed using version 2 (v2.2.0 beta) of the PICRUST (Phylogenetic Investigation of Communities by Reconstruction of Unobserved States) software package (Douglas et al., 2020). All OTU sequences were de-gapped and placed in a reference taxonomic tree based on the Integrated Microbial Genomes database. EPA-ng and GAPPA tools were used to determine the best position of these placed OTUs in the reference phylogeny (Barbera et al., 2019; Czech and Stamatakis, 2019; <http://www.hmmerr.org>, last access: 19 January 2021) after which KEGG orthologues for key enzymes involved in dark CO₂ fixation were predicted for each OTU. Using the derived KEGG Orthology (KO) numbers for different key genes for CO₂ fixation, the six known autotrophic pathways were deduced for all samples as previously done (Akinyede et al., 2022a, 2020). These include the Calvin–Benson–Bassham (CBB) pathway (or Calvin cycle), the reductive citric acid (rTCA) pathway, the Wood–Ljungdahl pathway (WLP), the 3-hydroxypropionate–methyl-CoA (3HP) cycle, the 3-hydroxypropionate–4-hydroxybutyrate (HP/HB) cycle, and the dicarboxylate–4-hydroxybutyrate (DC/HB) cycle.

Based on PICRUST2 predictions, the abundance of functional genes belonging to two CO₂ fixation pathways, the Calvin cycle and the rTCA pathway, were determined by quantitative PCR for the bulk soil as well in all soil samples incubated at 4 and 14 °C. Gene abundance of bacterial *16S rRNA*, RuBisCO marker genes (*cbbL* IA, *cbbL* IC, *cbbM*) for the Calvin–Benson–Bassham cycle and ATP citrate lyase genes, and *aclA* belonging to the reductive citric acid cycle was determined by quantitative PCR (qPCR) on the CFX96 Touch Real-Time PCR system (Bio-Rad, Singapore) using Maxima SYBR Green Master Mix (Agilent, CA, USA). Primer pair Bac 8Fmod–Bac 338R was used to target the *16S rRNA* genes (Loy et al., 2002; Daims et al., 1999), while F-*cbbL* IA–R-*cbbL* IA, F-*cbbL* IC–R-*cbbL* IC, and F-*cbbM*–R-*cbbM* were used to target both the form-I (*cbbL* IA and *cbbL* IC) and form-II (*cbbM*) RuBisCO marker genes (Alfreider et al., 2012, 2003), which is specific to both obligate and facultative chemolithoautotrophic bacteria groups like Proteobacteria (Selesi et al., 2005). Primer pair F-g-acl-Nit–R-g-acl-Nit was used to target the alpha subunit of the ATP citrate lyase (*aclA*) gene, which is specific to nitrite-oxidizing bacteria and complete ammonia-oxidizing (comammox) bacteria, e.g. *Nitrospira* (Alfreider et al., 2018). All cycling conditions and standards used for quantification are found in Akinyede et al. (2020) and Herrmann et al. (2012, 2015). Due to the absence of a reliable standardized qPCR protocol and primer sets to target genes for the WLP and the rest of the other autotrophic pathways, the presence of these pathways was based only on the predictions by PICRUST2.

2.8 Statistical analysis

We compared the CO₂ fixation rates per gram of soil and per gram of MBC between all soil samples incubated at 4 and 14 °C using Student's *t* test. To compare the respective Q_{10} values between the beech and spruce profile and across individual horizons, analysis of covariance (ANCOVA) and one-way ANOVA with Tukey's test were conducted, respectively. To compare other parameters between the beech and spruce soil profiles, e.g. net soil respiration rates between 4 and 14 °C and ¹³C signal of SOC and MBC, ANCOVA was also conducted. When comparing parameters between the beech and spruce soils using ANCOVA, soil depth also accounted for the variability in the measured parameters and was used as the covariate in the analysis. When deriving the CO₂ fixation and net soil respiration rates under projected future temperatures increase (from 8 to 12 °C), the mean Q_{10} values for the beech and spruce profiles were used in the Q_{10} equation described in Eq. (6) of the method in Sect. 2.5. As rates at 4 °C were low and, in some samples, below the detection limit (e.g. net respiration rates at the beech soil BvT depth), the rates per gram of soil measured at 14 °C were used (as k_2 , T_2) in the Q_{10} equation to derive rates at 8 °C (k_1 , T_1). The derived rates at 8 °C were then used (as k_1 , T_1) for the subsequent derivation of rates at 12 °C (k_2 , T_2).

Following Geyer et al. (2020), we quantified the proportion of excess ¹³C transferred into the SOC pool from the MBC pool via microbial residues as the total amount of excess ¹³C fixed in the SOC pool minus the excess ¹³C fixed in the intact MBC pool.

The variations in the bacterial community between the beech and spruce soil and with temperature were determined by measuring the beta diversity. Beta diversity was measured by performing principal coordinate analysis (PCoA) based on Bray–Curtis dissimilarity using the package *vegan* contained in R (Oksanen et al., 2008). Here, the bacterial communities from all beech and spruce soil samples were clustered based on their similarity and dissimilarity between the soils and with temperature. To determine the significance of the factors accounting for OTU variances shown in the PCoA plot between the two soils, across individual soil depth, and between temperatures, permutational multivariate analysis of variance (PERMANOVA) was performed with 999 permutations using “*adonis*” functions. Differences in the abundance of all predicted and quantified CO₂ fixation genes between the beech and spruce soil were analysed using ANOVA and Tukey’s test. For all statistical tests, differences with $p < 0.05$ were considered statistically significant. All statistical analyses were conducted with the R environment (v.3.6.1) and RStudio (v1.1.463).

3 Results

3.1 Effects of temperature on dark CO₂ fixation rates in beech and spruce soils

All soil incubations exposed to ¹³CO₂ were significantly enriched in δ¹³C relative to the controls at both 4 and 14 °C, indicating dark CO₂ fixation (Fig. S1 in the Supplement). In the top depths of both the beech and the spruce soils, significantly higher CO₂ fixation rates were observed at 14 °C than at 4 °C. For the top AB horizon of the beech soil, CO₂ fixation rates expressed in relation to soil dry weight (μg C g⁻¹ (dw) soil d⁻¹) (Fig. 1a) were almost 2 times higher with $0.033 \pm 0.006 \mu\text{g C g}^{-1} (\text{dw}) \text{ soil d}^{-1}$ at 14 °C compared to $0.018 \pm 0.006 \mu\text{g C g}^{-1} (\text{dw}) \text{ soil d}^{-1}$ at 4 °C ($p = 0.04$; Student’s *t* test). Similarly, the top AB depth of the spruce soil also featured ~ 2 times higher fixation rates at 14 °C with $0.030 \pm 0.003 \mu\text{g C g}^{-1} (\text{dw}) \text{ soil d}^{-1}$ than at 4 °C with $0.014 \pm 0.002 \mu\text{g C g}^{-1} (\text{dw}) \text{ soil d}^{-1}$ ($p = 0.005$). In the lower depths, however, no significant differences in fixation rates expressed per gram of soil dry weight were observed between soils incubated at 4 and 14 °C for either the beech soils ($p = 0.3$ and $p = 0.6$ at the Bv and BvT horizons, respectively) or the spruce soils ($p = 0.2$ and $p = 0.4$ at the Bv and BvT horizons, respectively). While we observed an expected decrease in fixation rates per gram of soil with depth in both soils due to the decreasing SOC content, there were no significant differences in rates between

the beech and spruce soil, neither at 4 nor at 14 °C. Across the depth profiles, changes in rates with temperature did not differ between the spruce (1.5–3.2-fold changes) and the beech soil (0.9–2.7-fold changes) ($p = 0.08$) as both soils showed a 70 %–90 % increase in the ¹³C signal with temperature (Fig. S1).

When expressed in relation to microbial biomass carbon (MBC), dark CO₂ fixation rates in the top AB horizon of the spruce soil were 1.6 times higher at 14 °C with $145.95 \pm 27.13 \mu\text{g C g}^{-1} \text{ MBC d}^{-1}$ than at 4 °C with $88.29 \pm 17.12 \mu\text{g C g}^{-1} \text{ MBC d}^{-1}$ ($p = 0.04$) (Fig. 1b). For the beech soil, however, values in the top AB depth were similar at 4 and 14 °C ($p = 0.3$) with 108.18 ± 8.82 and $125.11 \pm 23.76 \mu\text{g C g}^{-1} \text{ MBC d}^{-1}$, respectively. In the lower horizons, no significant differences between temperature treatments were observed for the two soils. Rates expressed per gram of MBC were approximately constant with depth, excepting the BvT horizon of the beech soil, which had lower rates. Taken together across depth profiles, stronger differences with temperature were observed for the spruce (1.3–2.6-fold changes) than the beech soil (0.9–1.4-fold changes) ($p = 0.003$). These differences in rates reflect the observed difference in the ¹³C signals of MBC with temperature between the soils. While up to a 124 % increase in the ¹³C signal of MBC was found for the spruce soil, the beech soil showed no more than a 23 % increase in the ¹³C signal of MBC with temperature (Fig. S1). These differences between the beech and spruce soil suggest that drivers of dark CO₂ fixation may differ between soils.

3.2 Q₁₀ of dark CO₂ fixation rates for beech and spruce soil profiles

The Q₁₀ values, the factor by which CO₂ fixation rates differed with the 10 °C rise in temperature, were 1.81 ± 0.17 across depths (for rates per gram of soil) for the beech soil, and 2.34 ± 0.21 for the spruce soil (Fig. 2a) with a mean Q₁₀ value of 2.07 ± 0.34 for all beech and spruce soils. Both the beech and the spruce soils showed large variability in the Q₁₀ values with depth with values ranging from 1.97 ± 0.84 at the AB depth and 1.63 ± 0.86 at the bottom BvT depth of the beech soil to 2.11 ± 0.07 and 2.53 ± 0.70 through the spruce soil profile. Thus, no significant differences between corresponding depths of both soil profiles were observed ($p = 0.81$, $p = 0.32$, and $p = 0.23$ for the AB, Bv, and BvT horizons, respectively). However, differing trends across individual depths for the beech and spruce soil were observed, with Q₁₀ values decreasing with depth in beech soil but increasing with depth in spruce soil ($R^2 = 0.92$, $p = 3.2 \times 10^{-8}$, ANCOVA).

We also calculated the Q₁₀ for rates per gram of MBC, as the microbial cells are responsible for dark CO₂ fixation and should be primarily affected by temperature. Compared to the Q₁₀ based on soil dry weight, the Q₁₀ based on MBC was lower in the beech soil ($p = 0.008$), which is linked to

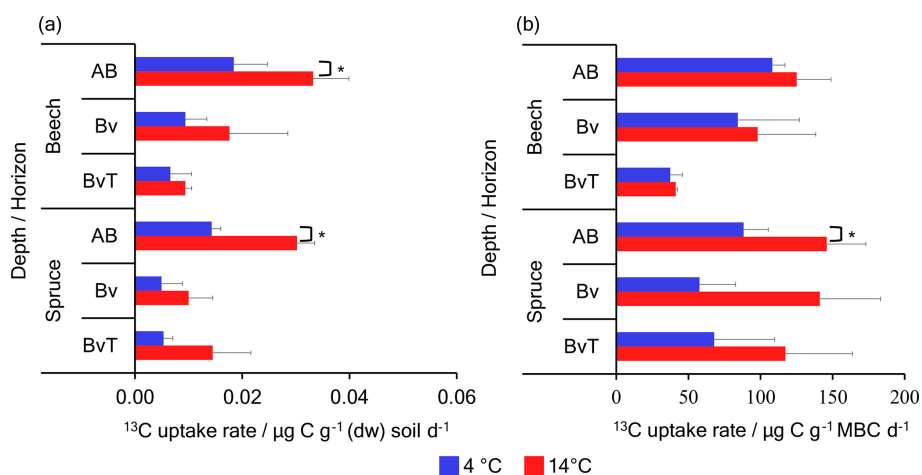


Figure 1. Dark CO₂ fixation rate measured from soil microcosms supplemented with 2 % ¹³CO₂ at 4 and 14 °C. Shown are (a) ¹³C uptake rates in soil expressed in µg C g⁻¹ (dw) soil d⁻¹ (micrograms of carbon per gram dry weight (dw) of soil per day) and (b) ¹³C uptake rates into MBC expressed in µg C g⁻¹ MBC d⁻¹ (micrograms of carbon per gram of microbial biomass carbon per day) after 21 d of incubation with 2 % ¹³CO₂ at 4 (blue bars) and 14 °C (red bars) across three horizons of the beech and spruce soils. Error bars indicate the standard deviation of incubations from three replicate soil cores. * denotes $p < 0.05$.

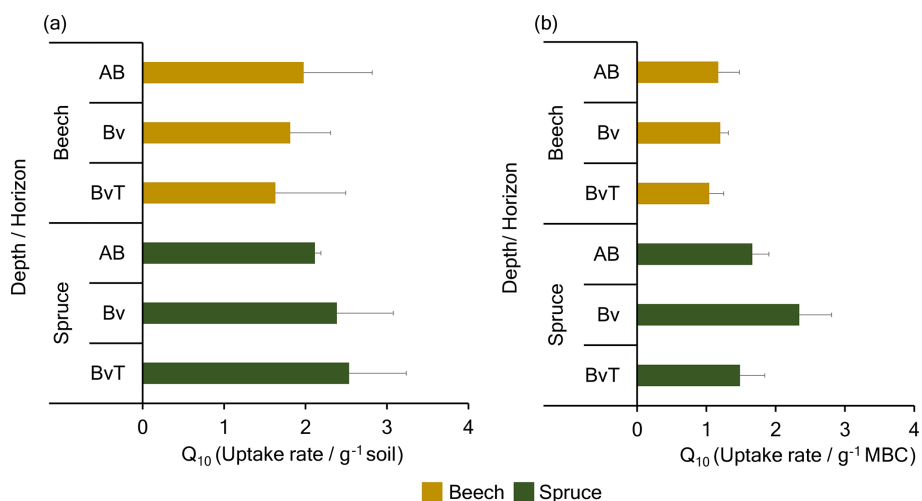


Figure 2. Temperature sensitivity (Q_{10}) of dark CO₂ fixation rate measured from soil microcosms supplemented with 2 % ¹³CO₂ at 4 and 14 °C. Shown are the Q_{10} (temperature sensitivity) values of dark CO₂ fixation rates derived from fixation rates expressed in (a) µg C g⁻¹ (dw) soil d⁻¹ (micrograms of carbon per gram dry weight (dw) of soil per day) and in (b) µg C g⁻¹ MBC d⁻¹ (micrograms of carbon per gram of microbial biomass carbon per day) after 21 d of incubation with 2 % ¹³CO₂ across three horizons in the beech and spruce soils.

the smaller differences in the ¹³C signal of MBC and calculated CO₂ fixation rates with temperature. For the spruce soil, no difference between the Q_{10} based on MBC and the Q_{10} based on soil dry weight was observed ($p = 0.13$). As a result, the spruce soil profile featured a higher mean Q_{10} based on rates per gram of MBC with 1.9 ± 0.63 (Fig. 2b) than the beech soil profile with 1.1 ± 0.20 across depth ($p = 0.003$; ANOVA and Tukey's test).

3.3 Allocation of ¹³C in the beech and spruce soils

As both the fixation rates and Q_{10} values differed between the beech and spruce soil, we aimed to determine if this was reflected by differences in the partitioning or transfer of the fixed ¹³C via microbial residues between the MBC and SOC pools. On average, the ¹³C signals of the MBC pool were significantly lower across the beech soil profile compared to the spruce soil profile at 14 °C ($R^2 = 0.91$, $p = 5.24 \times 10^{-8}$, ANCOVA) with no clear difference observed between forest types at 4 °C (Fig. S2 in the Supplement). In contrast, the ¹³C

signatures measured in SOC were on average higher in the beech than in the spruce soil across depth for soils incubated both at 4 and at 14 °C ($R^2 = 0.98$ and $p = 3.90 \times 10^{-12}$ for 4 °C and $R^2 = 0.96$ and $p = 1.05 \times 10^{-10}$ for 14 °C, ANCOVA). As a result, a higher proportion of fixed ¹³C was found to be allocated to the MBC pool in the spruce soil with up to 64 % compared to the beech soil with up to 32 % (Fig. 3). Hence, in the beech soil, a greater amount of ¹³C allocation into the SOC pool was observed compared to the spruce soil. In general, higher temperatures were associated with a larger increase in ¹³C allocation to SOC compared to MBC pools in the beech and spruce soils (Fig. 3). For instance, at the AB depth of the beech soil, ¹³C fixed into SOC increased from 67 % to 81 %, and in the spruce soil, it went up from 36 % to 63 %.

3.4 Effects of temperature on net soil respiration rates

In addition to the CO₂ fixation rates, we also determined net soil respiration rates during the preincubation phase. As expected, net respiration rates across all beech and spruce soil samples were 20–70 times higher than CO₂ fixation rates ($p = 0.005$) with values as high as 2.89 ± 1.26 and $2.31 \pm 0.9 \mu\text{g C g}^{-1}$ (dw) soil d⁻¹ at 14 °C at the top AB horizon of the beech and spruce soils, respectively. Net respiration rates were higher in all soils incubated under 14 °C than at 4 °C for both the beech ($R^2 = 0.73$, $p = 0.03$, ANCOVA) and spruce ($R^2 = 0.58$, $p = 0.02$, ANCOVA) profiles (Fig. 4). As rates were highly variable across replicates, no significant differences between the beech and the spruce soil or with depth were observed.

In response to warming, the Q_{10} values of net respiration rates per gram of soil for the beech and spruce soils were 2.87 ± 0.81 and 3.06 ± 0.78 , respectively. Taken together, the mean Q_{10} for net respiration rates across the beech and spruce soil profiles at 2.98 ± 0.69 was significantly higher than the Q_{10} of fixation rates relative to soil dry weight ($R^2 = 0.95$, $p = 3.0 \times 10^{-5}$, ANCOVA). Values ranged between 2.29 ± 0.004 and 3.44 ± 1.43 across the two AB and Bv depths in the beech soil and between 2.60 ± 0.12 and 3.96 ± 3.38 across all three depths of the spruce soil. Due to the high variations in net respiration rates among the soil samples, the Q_{10} values did not differ significantly between the beech and spruce soil and across the individual depth profiles. As net respiration rates were much higher than CO₂ fixation rates, the derived decomposition rates were nearly the same as the net respiration rates for the beech and spruce soils. Hence the Q_{10} values were also similar, having a mean value of 2.95 ± 1.34 (Table S3 in the Supplement).

3.5 Bacterial communities of the Hummelshain forest soils

The lower ¹³C allocation in MBC but higher allocations to SOC for beech than for spruce soils indicated a higher

turnover of fixed ¹³C from MBC to SOC in the beech soil compared to the spruce soil. We thus further checked if this higher turnover was accompanied by differences in the overall bacterial community composition and abundance. We investigated the *16S rRNA* gene amplicons at OTU level and determined *16S rRNA* gene copies by qPCR (Table 1 and Fig. S3 in the Supplement). Principal coordinate analysis (PCoA) revealed differences in the composition between the beech and spruce soil ($R^2 = 0.23$, $p = 0.001$, PERMANOVA, Fig. 5a). This was most pronounced in the top AB horizon ($R^2 = 0.67$, $p = 0.003$). Furthermore, the bacterial community composition also differed with soil depth ($R^2 = 0.30$, $p = 0.001$). As expected, the microbial abundance decreased with depth in both soils (Table 1). However, no difference in the microbial abundance between soils was observed at comparable depths. With respect to temperature, no shifts in the community composition were found in either beech ($R^2 = 0.014$, $p = 0.99$) or spruce ($R^2 = 0.015$, $p = 0.98$) soils (Fig. 5b). Likewise, the microbial abundances did not differ with temperature (Table S2).

3.6 Abundance of genes for CO₂ fixation

Based on presumed differences in residue formation and in the community composition between the soils, we speculate that the potential key players in the beech soil were composed of a higher proportion of groups with faster life cycles when compared to the spruce soil. As the rich SOC content in forest soils generally promotes faster growth of heterotrophs over chemolithoautotrophs, we further hypothesized that the beech bulk soil contains lower fractions of autotrophs compared to the spruce soil. We used PICRUST2 to predict and quantify the genetic potential for CO₂ fixation in both soils to test this hypothesis. Predicted autotrophic OTUs made up ~ 11 % of the total bacterial community in all samples. Most of the autotrophic OTUs were predicted to possess genes affiliated with RuBisCO of the CBB pathway for CO₂ fixation, with ~ 9 %, while genes of the WLP and the rTCA pathway were predicted in ~ 2 % and 0.1 % of the OTUs, respectively. The spruce bulk soil featured higher abundances of OTUs predicted to possess the RuBisCO gene than the beech bulk soil (Fig. 6a), with significantly higher proportions in the AB horizon ($p = 0.007$).

Quantitative PCR of marker gene coding for the CBB (RuBisCO (*cbbl* IA, *cbbl* IC, *cbbl* M)) and the rTCA pathway (ATP citrate lyase alpha subunit (*acla*)) was performed to confirm the predicted potential for autotrophic CO₂ fixation. Of the detected gene variants, the *cbbl* IC gene was the most abundant with up to 5 % of the bacterial *16S rRNA* gene copies in both soils, whereas other RuBisCO and *acla* genes constituted less than 1 % (Fig. S4 in the Supplement). The proportions of *cbbl* IC genes across the depths were significantly higher in the spruce than in the beech soil at 4 and 14 °C ($p = 0.007$, $p = 1.03 \times 10^{-6}$, respectively) (Fig. 6b).

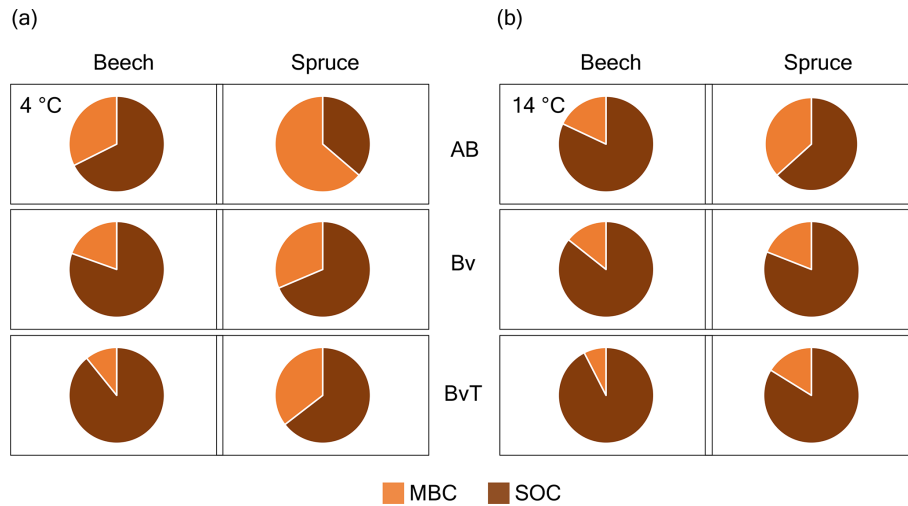


Figure 3. Proportion of fixed carbon recovered in MBC and SOC pools of the beech and spruce soils. The pie charts show the relative proportions of microbially derived ¹³CO₂ into MBC (orange fractions) and SOC (brown fractions) pools expressed as a percentage of the total fixed carbon after 21 d of incubation with 2% ¹³CO₂ for soils incubated at (a) 4 and (b) 14 °C across three horizons (AB, Bv, BvT) in beech and spruce soils. Values are the mean of three replicate incubations.

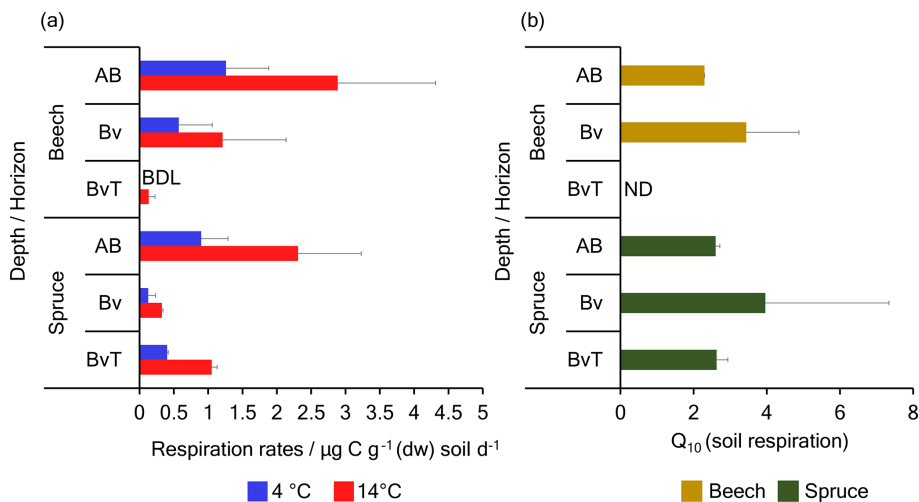


Figure 4. Net respiration rates and Q_{10} values measured from soil microcosms incubated at 4 and 14 °C. Shown are (a) net respiration rates in beech and spruce soils expressed in $\mu\text{g C g}^{-1}(\text{dw}) \text{ soil d}^{-1}$ (micrograms of carbon per gram dry weight (dw) of soil per day) at 4 (blue bars) and 14 °C (red bars) and (b) Q_{10} (temperature sensitivity) of net respiration rates measured after 4 d of preincubation in beech soils (yellow bars) and spruce soils (green bars) across depth. Error bars indicate the standard deviation of incubations from three replicate soil cores. BDL and ND denote values “below the detection limit” and values “not determined”, respectively.

In the bulk soil, however, this was only observed in the BvT horizon ($p = 0.03$).

4 Discussion

This study shows that the derived Q_{10} values of dark CO₂ fixation rates per gram of soil, with a mean value of 2.07 across the beech and spruce soil depths, were significantly lower than the average Q_{10} of net soil respiration rates per gram of soil with 2.98 for both soils, which suggests that soil

respiration is more sensitive to warming than CO₂ fixation. Our Q_{10} values of net soil respiration rates fall in the range of those reported for agricultural soils (1.5) and temperate mixed forest soils (3.1) (Fang et al., 2005; Conant et al., 2008; Hicks Pries et al., 2017; Li et al., 2021). For Q_{10} values of dark CO₂ fixation rates, a similar value of ~ 2.5 was extrapolated for afro-temperate forest soils (Nel and Cramer, 2019).

Comparing the responses of dark CO₂ fixation and net soil respiration to temperature for the same soil is important in

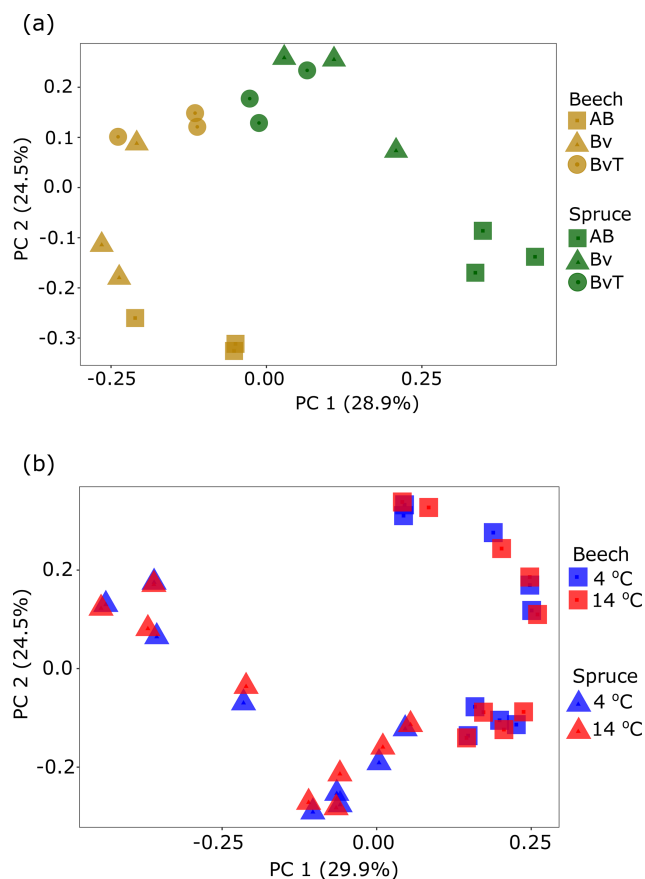


Figure 5. Bacterial community composition and community structure from beech and spruce bulk soil. Shown are the bacterial community structure of (a) the beech (yellow symbols) and spruce (green symbols) bulk soils before incubation and of (b) beech and spruce soils incubated with 2 % ¹³CO₂ at 4 (blue symbols) and 14 °C (red symbols). PCoA plots are based on OTU level analysis (Bray–Curtis dissimilarity) of *16S rRNA* gene amplicons generated by Illumina MiSeq sequencing with three independent data points per depth obtained from beech and spruce soils.

understanding the dynamics of SOC fluxes within the context of global climate change. Since dark CO₂ fixation can recycle up to 4 % of CO₂ respired from temperate forest soils (Spohn et al., 2019), higher CO₂ fixation rates might as well be affecting the magnitude of SOC losses from temperate forest soils under warming. By assuming a Q_{10} of 2.07 and 2.98 for dark CO₂ fixation rate and net soil respiration rates, respectively, we extrapolated the effect of future warming on the forest SOC fluxes. With a 4 °C increase in mean annual temperate forest soil temperature (~ 8 now to 12 °C by 2100) to 1 m deep by the end of this century (IPCC, 2013; Soong et al., 2020), dark CO₂ fixation rates to 1 m depth would increase by 33 % while net soil respiration rates would increase by 55 %. This indicates that future increase in net soil respiration might be 1.16 times higher than CO₂ fixation upon 4 °C warming. Hence, the potential for dark CO₂ fixation to recy-

cle or modulate carbon respired from temperate forest soils could decrease under future warming scenarios. However, the temperature response of dark CO₂ fixation and respiration in soils is likely also affected by varying temperatures occurring in different temperate forest biomes. Differences in carbon allocation between MBC and SOC also show that not all components of the soil carbon cycle will have the same response to soil temperature changes. Furthermore, higher temperature might alter primary production and root exudation, resulting in changes in soil carbon inputs and, consequently, soil pore space CO₂ concentrations and effluxes (Jakoby et al., 2020; Way and Oren, 2010; Yin et al., 2013). Thus, the estimates presented here are associated with a range of uncertainty.

Our measured soil CO₂ production in all soil incubations does not represent decomposition rates but the net soil respiration rates, as these rates include the effects of temperature on both CO₂ production (decomposition) and CO₂ fixation, with both processes occurring simultaneously (Braun et al., 2021). Thus, to accurately derive the decomposition rates, CO₂ fixation rates have to be added to measured net soil respiration rates. Although our measured CO₂ fixation rates were very small with only marginal effects on the Q_{10} of soil CO₂ production, that is, a Q_{10} of 2.98 vs. 2.95 for net soil respiration and decomposition rate, respectively, dark CO₂ fixation may result in an overestimation of Q_{10} of decomposition rates if only net soil respiration is measured. This is especially the case in scenarios where high CO₂ fixation rates are expected.

Unexpectedly, the two soils, beech and spruce, showed differences in their temperature response. Although Q_{10} values for CO₂ fixation rates per gram of soil were similar between the beech and spruce topsoil, the Q_{10} values differed in their depth trends, with decreasing Q_{10} with depth in the beech soil and increasing Q_{10} with depth in the spruce soil. Furthermore, while both soils showed similar temperature responses in terms of rates of CO₂ production per gram of soil, the temperature effect of CO₂ fixation rates expressed per gram of MBC was smaller in the beech than in the spruce soil. The lower Q_{10} in the beech soil was accompanied by higher proportions of newly fixed ¹³C in the SOC pool but lower proportions in the MBC pool when compared to the spruce soil, especially for soils incubated at 14 °C. This suggested that there was a higher transfer of microbially derived carbon from the MBC pool into the SOC pool in the beech soil. Through microbial residue formation, fixed ¹³C is transferred from the MBC into the SOC pool (Geyer et al., 2020; Miltner et al., 2012). A higher rate of residue formation in the beech soil will lead to a lower fraction of fixed ¹³C remaining in the MBC pool and, thereby, an underestimation of the CO₂ fixation rates per gram of MBC when compared to the spruce soil. Hence, a higher rate of microbial residue transfer in our 21 d incubations might explain the lower Q_{10} of fixation rates per gram of MBC in the beech than in the spruce soil. Such rapid residue formation is not uncommon in soils

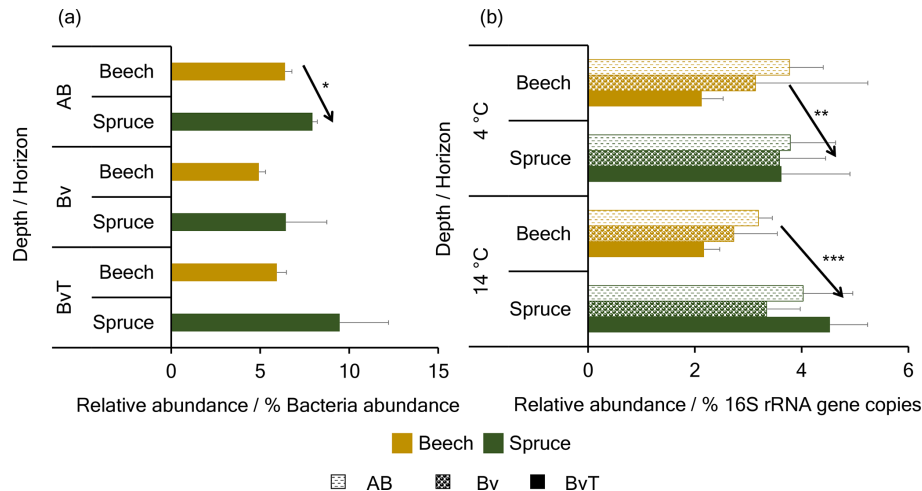


Figure 6. Relative abundance of RuBisCO genes in the beech and spruce soil. Shown are the relative abundances of (a) predicted and (b) quantified RuBisCO genes coding for the CBB pathway in the beech and spruce soil. Data in (a) are based on predictions by PICRUSt2 analysis of bacterial *16S rRNA* gene amplicon sequence data for the beech and spruce bulk soil, while data in (b) are acquired by qPCR of *cbbL* IC genes for both soils incubated at 4 and 14 °C. *, **, and *** denote $p < 0.05$, $p < 0.01$, and $p < 0.001$, respectively.

as it was observed in as little as 6 h in a temperate forest soil (Geyer et al., 2020). Microbial biomass can also turn over as necromass within a few days to weeks in soils (Kästner et al., 2021; Miltner et al., 2012) with turnover times of 18–21 d reported in agricultural soils (Cheng, 2009) and 33 d in temperate forest soils (Spohn et al., 2016). Thus, the formation of microbial residues can be observed within the timescale of our incubation experiment.

Accelerated microbial residue formation in the beech compared to the spruce soil might have been related to differences in soil abiotic parameters, in particular, factors differentially affecting either the lifespan (turnover) of microbial cells or the formation of extracellular metabolites from living cells. The biggest difference between the soils was soil texture, with lower clay and higher sand content in the beech compared to the spruce soil. Soil texture is known to affect microbial biomass turnover in soils (Van Veen et al., 1984; Sakamoto and Hodono, 2000; Prévost-Bouré et al., 2014), with high-clay-content soils often associated with slow biomass turnover into necromass compared to low-clay-content soils (Ali et al., 2020; Gregorich et al., 1991; Van Veen et al., 1985) due to the capacity of clay-rich soils to protect or preserve microbial cells, reducing overall the death rate (Van Veen et al., 1985, 1984). Interaction of microbial biomass with the negatively charged clay mineral particles was suggested as the mechanism causing biomass stability (Ali et al., 2020; Six et al., 2006). Clay–microbe interactions may promote microbial growth by maintaining an optimal pH range (Stotzky and Rem, 1966) and helping to adsorb metabolites inhibitory to microbial growth (Martin et al., 1976). The fine particles and small pore space characteristic of clay-rich soils also lead to a higher water-holding capacity (Fan et al., 2004; Jommi and Della Vecchia, 2016;

Miltner et al., 2009; Tsubo et al., 2007), resulting in the observed higher moisture content in the spruce compared to the beech soil. This higher moisture typical of clay-rich soils might partly be responsible for protecting microbes against moisture limitations when compared to sandy soils (Meisner et al., 2018; Schnürer et al., 1986; Bitton et al., 1976). Furthermore, small pores also restrict the access of higher organisms like protozoa, providing protection against predation (Elliott et al., 1980; Rutherford and Juma, 1992). Microbial protection promotes recycling or transfer of microbial extracellular products among the living communities, thus preventing further release into the soil pool (Gregorich et al., 1991). All of these mechanisms imply that the formation of microbial residues in the more clay-rich spruce soils should be slower than in the beech soil, as we observed. Due to the presence of larger mineral surface areas of clay in the spruce soils, association with clay surfaces can also lower residue formation and the amount of ¹³C label transferred would be a smaller proportion of total SOC. However, as the mineral composition of the soils was not measured, we cannot verify this assumption.

The higher microbial residue formation in the beech soil was accompanied by a different community composition and a lower proportion of genes for chemolithoautotrophic CO₂ fixation. Considering that both soils featured a similar abundance of the total bacterial community, this implied a higher proportion of heterotrophs among the beech soil communities. Growth of heterotrophs is favoured by high quantities of simple and complex carbon substrates released as root exudates (Huang et al., 2022; Li et al., 2018; Lladó et al., 2017; Vijay et al., 2019), whereas soils are usually deficient in reduced inorganic compounds (Jones et al., 2018) required as energy sources for autotrophic growth (Brock et al., 2003;

Berg, 2011). The redox potential of half reactions utilized by chemolithoautotrophs for energy often leads to lower energy yield than commonly observed for heterotrophs, causing chemolithoautotrophs to grow more slowly (Hooper and DiSpirito, 2013; Madigan et al., 2015; In't Zandt et al., 2018). As cell growth correlates with microbial residue formation (Geyer et al., 2020; Hagerty et al., 2014; Kästner et al., 2021), it is likely that heterotrophs in soils also form residues at faster rates than their chemolithoautotrophic counterparts. Hence, the suggested higher proportion of heterotrophs in the beech soil could also explain the higher rate of microbial residue formation observed when compared to the spruce soil. In both the beech and the spruce soil, the majority of the chemolithoautotrophic genes were affiliated to facultative autotrophs or mixotrophs which can also utilize SOC as a carbon source for growth (Yuan et al., 2012). This versatility allows them to be more active or grow faster than obligate autotrophs (Madigan et al., 2015). Hence, mixotrophs might contribute to microbial residue formation into the SOC pool especially in the beech soils.

The proportion of labelled carbon transferred to the SOC pool increased with temperature in both beech and spruce soils and across all depths, indicating higher inputs of microbial residues under warming. Higher temperatures have been often reported to increase inputs of microbial residues into soil (Ding et al., 2019; Hagerty et al., 2014; Li et al., 2019). Increasing soil temperature by 10 °C (15 to 25 °C) has been reported to double the specific death rate of microbial communities in soil due to increased protein turnover (Joergensen et al., 1990). Increased microbial residue formation of soil microbial biomass has been suggested to result from higher rates of enzymatic activities or changes in the abundance and composition of the soil microbial community (Ding et al., 2019; Hagerty et al., 2014). However, we did not find changes in the composition and abundance of the microbial community with warming in both the beech and the spruce soils during this short incubation time. Previous studies have shown that even after 4 or 5 years of warming, no increase in bacterial and fungal biomass is observed for a temperate forest soil (Schindlbacher et al., 2011) and it can take up to a decade to detect temperature-related changes in the soil community composition (Rinnan et al., 2009, 2007). In agreement, DeAngelis et al. (2015) revealed that 5 °C soil warming had a significant impact on bacterial community structure in mixed deciduous temperate forest soils only after 20 years of warming. Some authors have suggested that soil communities are more likely driven by gradual warming-induced changes in aboveground plant biomass and composition and associated shifts in carbon substrate, moisture, and nutrient conditions rather than just by elevated soil temperature effects (Sarathchandra et al., 1989; Rinnan et al., 2007; Frey et al., 2008; DeAngelis et al., 2015). This indicates that increases in dark CO₂ fixation in temperate forest soils as a response to short-term warming may not be caused by an increased microbial abundance or a shift in community com-

position but likely by an increase in the formation and release of microbial residues.

5 Conclusion

In response to warming, we measured an average Q_{10} of 2.07 for CO₂ fixation rates per gram of soil across 1 m depth profiles for soils dominated by deciduous beech and coniferous spruce trees. As net soil respiration rates across depth displayed a higher mean Q_{10} of 2.98, we estimated that net soil respiration might increase 1.16-fold more than CO₂ fixation rates under projected warming scenarios of 4 °C. The observed higher ¹³C signatures in the SOC pool of the beech soil suggested higher microbial residue formation, and this was reflected in the lower Q_{10} values for CO₂ fixation rates per gram of microbial biomass for the beech than for the spruce soil. Also, the higher allocation of CO₂-derived carbon to the SOC pool at higher temperatures indicates that warming primarily results in an increased residue formation of microbial cells. Findings from this study indicate that dark CO₂ fixation in temperate forest soils might be less responsive to future warming than net respiration and, as a result, could recycle less CO₂ respired from temperate forest soils in the future than it does now.

Code availability. Data analysis was performed using only standard tests and plotting commands in R. These codes are available on request from the corresponding author.

Data availability. Raw data associated with this study can be accessed at <https://doi.org/10.17617/3.EFHWIY> (Akinyede et al., 2022b). Generated sequences obtained for all soil samples in this study are deposited in the NCBI Sequence Read Archive (SRA) database with accession numbers SAMN26148471, SAMN26148472, SAMN26148473, SAMN26148474, SAMN26148475, and SAMN26148476 under the BioProject accession number PRJNA607916 and submission SUB11118201 (<https://submit.ncbi.nlm.nih.gov/subs/biosample/SUB11118201/> overview, last access: 7 March 2022).

Supplement. The supplement related to this article is available online at: <https://doi.org/10.5194/bg-19-4011-2022-supplement>.

Author contributions. RA and KK planned the sampling campaign; RA carried out the campaign and performed the experiments and measurements; RA and MT analysed the data and wrote the manuscript draft. MS, ST, and KK reviewed and edited the manuscript.

Competing interests. The contact author has declared that none of the authors has any competing interests.

Disclaimer. Publisher's note: Copernicus Publications remains neutral with regard to jurisdictional claims in published maps and institutional affiliations.

Acknowledgements. We thank Beate Michalzik and Florian Achilles for providing us with useful information on the soil properties and the history of the study site. We are grateful to Marco Pöhlmann, Jens Wurlitzer, and Stefan Riedel for soil sampling and incubation set-ups. We wish to acknowledge the contributions of Iris Kuhlmann for her support with CFE, Armin Jordan for helping with gas measurements, and members of the routine measurements and analytical departments of the Max Planck Institute for Biogeochemistry, Jena.

Financial support. This study was jointly supported by the Max Planck Institute for Biogeochemistry, Jena (MPI BGC); the International Max Planck Research School for Global Biogeochemical Cycles, Jena (IMPRS-gBGC); Deutscher Akademischer Austauschdienst (DAAD); and the Collaborative Research Centre 1076 AquaDiva (CRC AquaDiva), Germany. Funding by the DFG under Germany's Excellence Strategy – EXC 2051 – Project ID 390713860 was also provided.

Review statement. This paper was edited by Akihiko Ito and reviewed by two anonymous referees.

References

- Achilles, F., Tischer, A., Bernhardt-Römermann, M., Heinze, M., Reinhardt, F., Makeschin, F., and Michalzik, B.: European beech leads to more bioactive humus forms but stronger mineral soil acidification as Norway spruce and Scots pine – Results of a repeated site assessment after 63 and 82 years of forest conversion in Central Germany, *Forest Ecol. Manag.*, 483, 118769, <https://doi.org/10.1016/j.foreco.2020.118769>, 2020.
- Adams, M. B., Kelly, C., Kabrick, J., and Schuler, J.: Temperate forests and soils, Chap. 6, in: *Global Change and Forest Soils: Cultivating stewardship of a finite natural resource. Developments in Soil Science*, edited by: Busse, M., Giardina, C. P., Morris, D. M., and Page, D. D. S., Elsevier, 36, 83–108, <https://doi.org/10.1016/b978-0-444-63998-1.00006-9>, 2019.
- Akinyede, R., Taubert, M., Schrupf, M., Trumbore, S., and Küsel, K.: Rates of dark CO₂ fixation are driven by microbial biomass in a temperate forest soil, *Soil Biol. Biochem.*, 150, 107950, <https://doi.org/10.1016/j.soilbio.2020.107950>, 2020.
- Akinyede, R., Taubert, M., Schrupf, M., Trumbore, S., and Küsel, K.: Dark CO₂ fixation in temperate beech and pine forest soils, *Soil Biol. Biochem.*, 165, 108526, <https://doi.org/10.1016/j.soilbio.2021.108526>, 2022a.
- Akinyede, R., Taubert, M., Schrupf, M., Trumbore, S., and Küsel, K.: Temperature sensitivity of dark CO₂ fixation in temperate forest soils, Edmond V1 [data set], <https://doi.org/10.17617/3.EFHWIY>, 2022b.
- Alfreider, A., Vogt, C., Hoffmann, D., and Babel, W.: Diversity of ribulose-1,5-bisphosphate carboxylase/oxygenase large-subunit genes from groundwater and aquifer microorganisms, *Microb. Ecol.*, 45, 317–328, <https://doi.org/10.1007/s00248-003-2004-9>, 2003.
- Alfreider, A., Schirmer, M., and Vogt, C.: Diversity and expression of different forms of RubisCO genes in polluted groundwater under different redox conditions, *FEMS Microbiol. Ecol.*, 79, 649–660, <https://doi.org/10.1111/j.1574-6941.2011.01246.x>, 2012.
- Alfreider, A., Grimus, V., Luger, M., Ekblad, A., Salcher, M. M., and Summerer, M.: Autotrophic carbon fixation strategies used by nitrifying prokaryotes in freshwater lakes, *FEMS Microbiol. Ecol.*, 94, 1–12, <https://doi.org/10.1093/femsec/fiy163>, 2018.
- Ali, R. S., Poll, C., and Kandeler, E.: Soil Properties Control Microbial Carbon Assimilation and Its Mean Residence Time, *Frontiers in Environmental Science*, 8, 1–9, <https://doi.org/10.3389/fenvs.2020.00033>, 2020.
- Arrhenius, S.: Über die Reaktionsgeschwindigkeit bei der Inversion von Rohrzucker durch Säuren, *Z. Phys. Chem.*, 4, 226–248, 1889.
- Barbera, P., Kozlov, A. M., Czech, L., Morel, B., Darriba, D., Flouri, T., and Stamatakis, A.: EPA-ng: Massively Parallel Evolutionary Placement of Genetic Sequences, *Syst. Biol.*, 68, 365–369, <https://doi.org/10.1093/sysbio/syy054>, 2019.
- Berg, I. A.: Ecological aspects of the distribution of different autotrophic CO₂ fixation pathways, *Appl. Environ. Microb.*, 77, 1925–1936, <https://doi.org/10.1128/AEM.02473-10>, 2011.
- Beulig, F., Urich, T., Nowak, M., Trumbore, S. E., Gleixner, G., Gilfillan, G. D., Fjelland, K. E., and Küsel, K.: Altered carbon turnover processes and microbiomes in soils under long-term extremely high CO₂ exposure, *Nat. Microbiol.*, 1, 1–9, <https://doi.org/10.1038/nmicrobiol.2015.25>, 2016.
- Bitton, G., Henis, Y., and Lahav, N.: Influence of clay minerals, humic acid and bacterial capsular polysaccharide on the survival of *Klebsiella aerogenes* exposed to drying and heating in soils, *Plant Soil*, 45, 65–74, 1976.
- Bormann, H.: Analysis of the suitability of the German soil texture classification for the regional scale application of physical based hydrological model, *Adv. Geosci.*, 11, 7–13, <https://doi.org/10.5194/adgeo-11-7-2007>, 2007.
- Braun, A., Spona-Friedl, M., Avramov, M., Elsner, M., Baltar, F., Reinthaler, T., Herndl, G. J., and Griebler, C.: Reviews and syntheses: Heterotrophic fixation of inorganic carbon – significant but invisible flux in environmental carbon cycling, *Biogeosciences*, 18, 3689–3700, <https://doi.org/10.5194/bg-18-3689-2021>, 2021.
- Brock, T. D., Madigan, M. T., Martinko, J. P., and Parker, J. (Eds.): *Brock Biology of Microorganisms*, 10th Edn., Prentice Hall, Upper Saddle River, New Jersey, 565–575, ISBN 0-13-049147-0, 2003.
- Cheng, W.: Rhizosphere priming effect: Its functional relationships with microbial turnover, evapotranspiration, and C-N budgets, *Soil Biol. Biochem.*, 41, 1795–1801, <https://doi.org/10.1016/j.soilbio.2008.04.018>, 2009.
- Conant, R. T., Drijber, R. A., Haddix, M. L., Parton, W. J., Paul, E. A., Plante, A. F., Six, J., and Steinweg, M. J.: Sensitivity of organic matter decomposition to warming varies with its quality, *Glob. Change Biol.*, 14, 868–877, <https://doi.org/10.1111/j.1365-2486.2008.01541.x>, 2008.

- Coplen, T. B., Brand, W. A., Gehre, M., Gröning, M., Meljer, L. H. A. J., Toman, B., and Verkouteren, R. M.: New Guidelines for delta ¹³C Measurements, *Anal. Chem.*, 78, 2439–2441, 2006.
- Czech, L. and Stamatakis, A.: Scalable methods for analyzing and visualizing phylogenetic placement of metagenomic samples, *PLoS ONE*, 14, 1–50, <https://doi.org/10.1371/journal.pone.0217050>, 2019.
- Daims, H., Brühl, A., Amann, R., Schleifer, K.-H., and Wagner, M.: The domain-specific probe EUB338 is insufficient for the detection of all Bacteria: development and evaluation of a more comprehensive probe set, *Syst. Appl. Microbiol.*, 22, 434–444, 1999.
- Davidson, E. A. and Janssens, I. A.: Temperature sensitivity of soil carbon decomposition and feedbacks to climate change, *Nature*, 440, 165–173, <https://doi.org/10.1038/nature04514>, 2006.
- DeAngelis, K. M., Pold, G., Topçuoğlu, B. D., van Diepen, L. T. A., Varney, R. M., Blanchard, J. L., Melillo, J., and Frey, S. D.: Long-term forest soil warming alters microbial communities in temperate forest soils, *Front. Microbiol.*, 6, 1–13, <https://doi.org/10.3389/fmicb.2015.00104>, 2015.
- Ding, X., Chen, S., Zhang, B., Liang, C., He, H., and Horwath, W. R.: Warming increases microbial residue contribution to soil organic carbon in an alpine meadow, *Soil Biol. Biochem.*, 135, 13–19, <https://doi.org/10.1016/j.soilbio.2019.04.004>, 2019.
- Dossa, G. G. O., Paudel, E., Wang, H., Cao, K., Schaefer, D., and Harrison, R. D.: Correct calculation of CO₂ efflux using a closed-chamber linked to a non-dispersive infrared gas analyzer, *Methods Ecol. Evol.*, 6, 1435–1442, <https://doi.org/10.1111/2041-210X.12451>, 2015.
- Douglas, G. M., Maffei, V. J., Zaneveld, J. R., Yurgel, S. N., James, R., Taylor, C. M., Huttenhower, C., and Langille, M. G. I.: PICRUSt2 for prediction of metagenome functions, *Nat. Biotechnol.*, 38, 685–688, <https://doi.org/10.1038/s41587-020-0548-6>, 2020.
- Dreiss, L. M. and Volin, J. C.: Forests: temperate evergreen and deciduous, in: *Encyclopedia of Natural Resources – Land – Volume 1*, edited by: Yeqiao, W., 1st Edn., CRC Press, 214–223, ISBN 9780203757628, 2014.
- Eckelmann, W., Sponagel, H., Grotenthaler, W., Hartmann, K.-J., Hartwich, R., Janetzko, P., Joisten, H., Kühn, D., Sabel, K.-J. and Traidl, R. (Eds.): *Bodenkundliche Kartieranleitung, KA5*, 5th Edn., Schweizerbart'sche Verlagsbuchhandlung, ISBN 978-3-510-95804-7, 2006.
- Edgar, R. C., Haas, B. J., Clemente, J. C., Quince, C., and Knight, R.: UCHIME improves sensitivity and speed of chimera detection, *Bioinformatics*, 27, 2194–2200, <https://doi.org/10.1093/bioinformatics/btr381>, 2011.
- Elliott, E. T., Anderson, R. V., Coleman, D. C., and Cole, C. V.: Habitable Pore Space and Microbial Trophic Interaction, *Oikos*, 35, 327–335, <https://doi.org/10.2307/3544648>, 1980.
- Erb, T. J.: Carboxylases in natural and synthetic microbial pathways, *Appl. Environ. Microb.*, 77, 8466–8477, <https://doi.org/10.1128/AEM.05702-11>, 2011.
- Fan, T. W. M., Lane, A. N., Chekmenev, E., Wittebort, R. J., and Higashi, R. M.: Synthesis and physicochemical properties of peptides in soil humic substances, *J. Pept. Res.*, 63, 253–264, <https://doi.org/10.1111/j.1399-3011.2004.00142.x>, 2004.
- Fang, C., Smith, P., Moncrieff, J. B., and Smith, J. U.: Similar response of labile and resistant soil organic matter pools to changes in temperature, *Nature*, 433, 57–59, <https://doi.org/10.1038/nature04044>, 2005.
- Frey, S. D., Drijber, R., Smith, H., and Melillo, J.: Microbial biomass, functional capacity, and community structure after 12 years of soil warming, *Soil Biol. Biochem.*, 40, 2904–2907, <https://doi.org/10.1016/j.soilbio.2008.07.020>, 2008.
- Geyer, K., Schnecker, J., Grandy, A. S., Richter, A., and Frey, S.: Assessing microbial residues in soil as a potential carbon sink and moderator of carbon use efficiency, *Biogeochemistry*, 151, 237–249, <https://doi.org/10.1007/s10533-020-00720-4>, 2020.
- Graser, H.: *Die Bewirtschaftung des erzgebirgischen Fichtenwaldes, Erster Band*, Hofbuchhandlung H. Burdach, Dresden, 1928.
- Gregorich, E. G., Voroney, R. P., and Kachanoski, R. G.: Turnover of carbon through the microbial biomass in soils with different texture, *Soil Biol. Biochem.*, 23, 799–805, [https://doi.org/10.1016/0038-0717\(91\)90152-A](https://doi.org/10.1016/0038-0717(91)90152-A), 1991.
- Hagerty, S. B., Van Groenigen, K. J., Allison, S. D., Hungate, B. A., Schwartz, E., Koch, G. W., Kolka, R. K., and Dijkstra, P.: Accelerated microbial turnover but constant growth efficiency with warming in soil, *Nat. Clim. Change*, 4, 903–906, <https://doi.org/10.1038/nclimate2361>, 2014.
- Herrmann, M., Hädrich, A., and Küsel, K.: Predominance of thaumarchaeal ammonia oxidizer abundance and transcriptional activity in an acidic fen, *Environ. Microbiol.*, 14, 3013–3025, <https://doi.org/10.1111/j.1462-2920.2012.02882.x>, 2012.
- Herrmann, M., Ruzsnyák, A., Akob, D. M., Schulze, I., Opitz, S., Totsche, K. U., and Küsel, K.: Large fractions of CO₂-fixing microorganisms in pristine limestone aquifers appear to be involved in the oxidation of reduced sulfur and nitrogen compounds, *Appl. Environ. Microb.*, 81, 2384–2394, <https://doi.org/10.1128/AEM.03269-14>, 2015.
- Hicks Pries, C. E., Castanha, C., Porras, R., Phillips, C., and Torn, M. S.: The whole-soil carbon flux in response to warming, *Science*, 355, 1420–1423, <https://doi.org/10.1126/science.aaa0457>, 2017.
- Hooper, A. B. and DiSpirito, A. A.: Chemolithotrophy, *Encyclopedia of Biological Chemistry*, 1, 486–492, <https://doi.org/10.1016/B978-0-12-378630-2.00219-X>, 2013.
- Huang, X., Duan, C., Yu, J., and Dong, W.: Transforming heterotrophic to autotrophic denitrification process: Insights into microbial community, interspecific interaction and nitrogen metabolism, *Bioresource Technol.*, 345, 126471, <https://doi.org/10.1016/j.biortech.2021.126471>, 2022.
- Hugelius, G., Strauss, J., Zubrzycki, S., Harden, J. W., Schuur, E. A. G., Ping, C.-L., Schirmer, L., Grosse, G., Michaelson, G. J., Koven, C. D., O'Donnell, J. A., Elberling, B., Mishra, U., Camill, P., Yu, Z., Palmtag, J., and Kuhry, P.: Estimated stocks of circumpolar permafrost carbon with quantified uncertainty ranges and identified data gaps, *Biogeosciences*, 11, 6573–6593, <https://doi.org/10.5194/bg-11-6573-2014>, 2014.
- Hügler, M. and Sievert, S. M.: Beyond the Calvin Cycle: Autotrophic Carbon Fixation in the Ocean, *Annu. Rev. Mar. Sci.*, 3, 261–289, <https://doi.org/10.1306/06210404037>, 2011.
- In't Zandt, M. H., de Jong, A. E., Slomp, C. P., and Jetten, M. S.: The hunt for the most-wanted chemolithoautotrophic spookmicrobes, *FEMS Microbiol. Ecol.*, 94, 1–17, <https://doi.org/10.1093/femsec/fiy064>, 2018.

- IPCC: Summary for Policymakers, in: *Climate Change – The Physical Science Basis. Contribution of Working Group I to the Fifth Assessment Report of the Intergovernmental Panel on Climate Change*, edited by: Stocker, T. F., Qin, D., Plattner, G.-K., Tignor, M., Allen, S. K., Boschung, J., Nauels, A., Xia, Y., Bex, V., and Midgley, P. M., Cambridge University Press, Cambridge, United Kingdom and New York, NY, USA, 20–23, <https://selectra.co.uk/sites/selectra.co.uk/files/pdf/Climate%20change%202013.pdf> (last access: 25 August 2022), 2013.
- IUSS Working Group WRB: World reference base for soil resources 2014, updated 2015, International soil classification system for naming soils and creating legends for soil maps, World Soil Resources Reports No. 106, <https://doi.org/10.1017/S0014479706394902>, 2015.
- Jakoby, G., Rog, I., Megidish, S., and Klein, T.: Enhanced root exudation of mature broadleaf and conifer trees in a Mediterranean forest during the dry season, *Tree Physiol.*, 40, 1595–1605, <https://doi.org/10.1093/treephys/tpaa092>, 2020.
- Jobbágy, E. G. and Jackson, R. B.: The vertical distribution of soil organic carbon and its relation to climate and vegetation, *Ecol. Appl.*, 10, 423–436, [https://doi.org/10.1890/1051-0761\(2000\)010\[0423:TVDOSO\]2.0.CO;2](https://doi.org/10.1890/1051-0761(2000)010[0423:TVDOSO]2.0.CO;2), 2000.
- Joergensen, R. G. and Mueller, T.: The fumigation-extraction method to estimate soil microbial biomass: Calibration of the kEN value, *Soil Biol. Biochem.*, 28, 33–37, [https://doi.org/10.1016/0038-0717\(95\)00101-8](https://doi.org/10.1016/0038-0717(95)00101-8), 1996.
- Joergensen, R. G., Brookes, P. C., and Jenkinson, D. S.: Survival of the soil microbial biomass at elevated temperatures, *Soil Biol. Biochem.*, 22, 1129–1136, [https://doi.org/10.1016/0038-0717\(90\)90039-3](https://doi.org/10.1016/0038-0717(90)90039-3), 1990.
- Joergensen, R. G., Wu, J., and Brookes, P. C.: Measuring soil microbial biomass using an automated procedure, *Soil Biol. Biochem.*, 43, 873–876, <https://doi.org/10.1016/j.soilbio.2010.09.024>, 2011.
- Jommi, C. and Della Vecchia, G.: Fabric and clay activity in soil water retention behaviour, *E3S Web Conf.*, 9, 04022, <https://doi.org/10.1051/e3sconf/20160904002>, 2016.
- Jones, R. M., Goordial, J. M., and Orcutt, B. N.: Low energy subsurface environments as extraterrestrial analogs, *Front. Microbiol.*, 9, 1–18, <https://doi.org/10.3389/fmicb.2018.01605>, 2018.
- Kaiser, K., Wemheuer, B., Korolkow, V., Wemheuer, F., Nacke, H., Schöning, I., Schrupp, M., and Daniel, R.: Driving forces of soil bacterial community structure, diversity, and function in temperate grasslands and forests, *Sci. Rep.-UK*, 6, 1–12, <https://doi.org/10.1038/srep33696>, 2016.
- Kästner, M., Miltner, A., Thiele-Bruhn, S., and Liang, C.: Microbial Necromass in Soils – Linking Microbes to Soil Processes and Carbon Turnover, *Frontiers in Environmental Science*, 9, 1–18, <https://doi.org/10.3389/fenvs.2021.756378>, 2021.
- Klindworth, A., Pruesse, E., Schweer, T., Peplies, J., Quast, C., Horn, M., and Glöckner, F. O.: Evaluation of general 16S ribosomal RNA gene PCR primers for classical and next-generation sequencing-based diversity studies, *Nucleic Acids Res.*, 41, 1–11, <https://doi.org/10.1093/nar/gks808>, 2013.
- Lal, R.: Soil carbon sequestration to mitigate climate change, *Geoderma*, 123, 1–22, <https://doi.org/10.1016/j.geoderma.2004.01.032>, 2004.
- Leifeld, J. and Fuhrer, J.: The temperature response of CO₂ production from bulk soils and soil fractions is related to soil organic matter quality, *Biogeochemistry*, 75, 433–453, <https://doi.org/10.1007/s10533-005-2237-4>, 2005.
- Li, B., Li, Z., Sun, X., Wang, Q., Xiao, E., and Sun, W.: DNA-SIP Reveals the Diversity of Chemolithoautotrophic Bacteria Inhabiting Three Different Soil Types in Typical Karst Rocky Desertification Ecosystems in Southwest China, *Microb. Ecol.*, 76, 976–990, <https://doi.org/10.1007/s00248-018-1196-y>, 2018.
- Li, H., Yang, S., Semenov, M. V., Yao, F., Ye, J., Bu, R., Ma, R., Lin, J., Kurganova, I., Wang, X., Deng, Y., Kravchenko, I., Jiang, Y., and Kuzyakov, Y.: Temperature sensitivity of SOM decomposition is linked with a K-selected microbial community, *Glob. Change Biol.*, 27, 2763–2779, <https://doi.org/10.1111/gcb.15593>, 2021.
- Li, J., Wang, G., Mayes, M. A., Allison, S. D., Frey, S. D., Shi, Z., Hu, X. M., Luo, Y., and Melillo, J. M.: Reduced carbon use efficiency and increased microbial turnover with soil warming, *Glob. Change Biol.*, 25, 900–910, <https://doi.org/10.1111/gcb.14517>, 2019.
- Liu, Z., Sun, Y., Zhang, Y., Feng, W., Lai, Z., Fa, K., and Qin, S.: Metagenomic and ¹³C tracing evidence for autotrophic atmospheric carbon absorption in a semiarid desert, *Soil Biol. Biochem.*, 125, 156–166, <https://doi.org/10.1016/j.soilbio.2018.07.012>, 2018.
- Lladó, S., López-Mondéjar, R., and Baldrian, P.: Forest Soil Bacteria: Diversity, Involvement in Ecosystem Processes, and Response to Global Change, *Microbiol. Mol. Biol. R.*, 81, 1–27, <https://doi.org/10.1128/MMBR.00063-16>, 2017.
- Long, X. E., Yao, H., Wang, J., Huang, Y., Singh, B. K., and Zhu, Y. G.: Community Structure and Soil pH Determine Chemoautotrophic Carbon Dioxide Fixation in Drained Paddy Soils, *Environ. Sci. Technol.*, 49, 7152–7160, <https://doi.org/10.1021/acs.est.5b00506>, 2015.
- Loy, A., Lehner, A., Lee, N., Adamczyk, J., Meier, H., Ernst, J., Schleifer, K. H., and Wagner, M.: Oligonucleotide microarray for 16S rRNA gene-based detection of all recognized lineages of sulfate-reducing prokaryotes in the environment, *Appl. Environ. Microb.*, 68, 5064–5081, 2002.
- Madigan, M. T., Martinko, J. M., Bender, K. S., Buckley, D. H., and Stahl, D. A. (Eds.): *Brock Biology of Microorganisms*, 14th Edn., Pearson Education, Inc, 79–83, ISBN 978-0-321-89739-8, 2015.
- Martens, R.: Current methods for measuring microbial biomass C in soil: Potentials and limitations, *Biol. Fert. Soils*, 19, 87–99, <https://doi.org/10.1007/BF00336142>, 1995.
- Martin, J., Filip, Z., and Haider, K.: Effect of Montmorillonite and Humate on Growth and Metabolic Activity of Some, *Soil Biol. Biochem.*, 8, 409–413, 1976.
- Meisner, A., Jacquiod, S., Snoek, B. L., Ten Hooven, F. C., and van der Putten, W. H.: Drought legacy effects on the composition of soil fungal and prokaryote communities, *Front. Microbiol.*, 9, 1–12, <https://doi.org/10.3389/fmicb.2018.00294>, 2018.
- Melillo, J. M., Stuedler, P. A., Aber, J. D., Newkirk, K., Lux, H., Bowles, F. P., Catricala, C., Magill, A., Ahrens, T., and Morrisseau, S.: Soil warming and carbon-cycle feedbacks to the climate system, *Science*, 298, 2173–2176, <https://doi.org/10.1126/science.1074153>, 2002.

- Melillo, J. M., Butler, S., Johnson, J., Mohan, J., Steudler, P., Lux, H., Burrows, E., Bowles, F., Smith, R., Scott, L., Vario, C., Hill, T., Burton, A., Zhou, Y. M., and Tang, J.: Soil warming, carbon-nitrogen interactions, and forest carbon budgets, *P. Natl. Acad. Sci. USA*, 108, 9508–9512, <https://doi.org/10.1073/pnas.1018189108>, 2011.
- Melillo, J. M., Frey, S. D., DeAngelis, K. M., Werner, W. J., Bernard, M. J., Bowles, F. P., Pold, G., Knorr, M. A., and Grandy, A. S.: Long-term pattern and magnitude of soil carbon feedback to the climate system in a warming world, *Science*, 358, 101–105, <https://doi.org/10.1126/science.aan2874>, 2017.
- Miltner, A., Richnow, H. H., Kopinke, F. D., and Kästner, M.: Assimilation of CO₂ by soil microorganisms and transformation into soil organic matter, *Org. Geochem.*, 35, 1015–1024, <https://doi.org/10.1016/j.orggeochem.2004.05.001>, 2004.
- Miltner, A., Kopinke, F. D., Kindler, R., Selesi, D., Hartmann, A., and Kästner, M.: Non-photosynthetic CO₂ fixation by soil microorganisms, *Plant Soil*, 269, 193–203, <https://doi.org/10.1007/s11104-004-0483-1>, 2005.
- Miltner, A., Kindler, R., Knicker, H., Richnow, H. H., and Kästner, M.: Fate of microbial biomass-derived amino acids in soil and their contribution to soil organic matter, *Org. Geochem.*, 40, 978–985, <https://doi.org/10.1016/j.orggeochem.2009.06.008>, 2009.
- Miltner, A., Bombach, P., Schmidt-Brücken, B., and Kästner, M.: SOM genesis: Microbial biomass as a significant source, *Biogeochemistry*, 111, 41–55, <https://doi.org/10.1007/s10533-011-9658-z>, 2012.
- Nel, J. A. and Cramer, M. D.: Soil microbial anaplerotic CO₂ fixation in temperate soils, *Geoderma*, 335, 170–178, <https://doi.org/10.1016/j.geoderma.2018.08.014>, 2019.
- Niederberger, T. D., Sohm, J. A., Gunderson, T., Tirindelli, J., Capone, D. G., Carpenter, E. J., and Cary, S. C.: Carbon-fixation rates and associated microbial communities residing in arid and ephemerally wet antarctic dry valley soils, *Front. Microbiol.*, 6, 1–9, <https://doi.org/10.3389/fmicb.2015.01347>, 2015.
- Nowak, M. E., Beulig, F., von Fischer, J., Muhr, J., Küsel, K., and Trumbore, S. E.: Autotrophic fixation of geogenic CO₂ by microorganisms contributes to soil organic matter formation and alters isotope signatures in a wetland mofette, *Biogeosciences*, 12, 7169–7183, <https://doi.org/10.5194/bg-12-7169-2015>, 2015.
- Ocio, J. A. and Brookes, P. C.: An evaluation of methods for measuring the microbial biomass in soils following recent additions of wheat straw and the characterization of the biomass that develops, *Soil Biol. Biochem.*, 22, 685–694, [https://doi.org/10.1016/0038-0717\(90\)90016-S](https://doi.org/10.1016/0038-0717(90)90016-S), 1990.
- Oksanen, J., Kindt, R., Legendre, P., O'Hara, B., Simpson, G. L., Solymos, P. M., Stevens, M. H. H., and Wagner, H.: The Vegan Package, *Community Ecology Package [code]*, 190, https://www.researchgate.net/profile/Gavin-Simpson-2/publication/228339454_The_vegan_Package/links/0912f50be86bc29a7f000000/The-vegan-Package.pdf (last access: 25 August 2022), 2008.
- Prévost-Bouré, N. C., Dequiedt, S., Thioulouse, J., Lelièvre, M., Saby, N. P. A., Jolivet, C., Arrouays, D., Plassart, P., Lemanceau, P., and Ranjard, L.: Similar processes but different environmental filters for soil bacterial and fungal community composition turnover on a broad spatial scale, *PLoS ONE*, 9, 1–11, <https://doi.org/10.1371/journal.pone.0111667>, 2014.
- Quast, C., Pruesse, E., Yilmaz, P., Gerken, J., Schweer, T., Yarza, P., Peplies, J., and Glöckner, F. O.: The SILVA ribosomal RNA gene database project: Improved data processing and web-based tools, *Nucleic Acids Res.*, 41, 590–596, <https://doi.org/10.1093/nar/gks1219>, 2013.
- Rastogi, M., Singh, S., and Pathak, H.: Emission of carbon dioxide from soil, *Curr. Sci. India*, 82, 510–517, 2002.
- Rinnan, R., Michelsen, A., Bååth, E., and Jonasson, S.: Fifteen years of climate change manipulations alter soil microbial communities in a subarctic heath ecosystem, *Glob. Change Biol.*, 13, 28–39, <https://doi.org/10.1111/j.1365-2486.2006.01263.x>, 2007.
- Rinnan, R., Stark, S., and Tolvanen, A.: Responses of vegetation and soil microbial communities to warming and simulated herbivory in a subarctic heath, *J. Ecol.*, 97, 788–800, <https://doi.org/10.1111/j.1365-2745.2009.01506.x>, 2009.
- Rutherford, P. M. and Juma, N. G.: Influence of soil texture on protozoa-induced mineralization of bacterial carbon and nitrogen, *Can. J. Soil Sci.*, 72, 183–200, <https://doi.org/10.4141/cjss92-019>, 1992.
- Sakamoto, K. and Hodono, N.: Turnover time of microbial biomass carbon in Japanese upland soils with different textures, *Soil Sci. Plant Nutr.*, 46, 483–490, 2000.
- Šantrůčková, H., Bird, M. I., Elhottová, D., Novák, J., Píček, T., Šimek, M., and Tykva, R.: Heterotrophic fixation of CO₂ in soil, *Microb. Ecol.*, 49, 218–225, <https://doi.org/10.1007/s00248-004-0164-x>, 2005.
- Šantrůčková, H., Kotas, P., Bárta, J., Urich, T., Čapek, P., Palmtag, J., Eloy Alves, R. J., Biasi, C., Diáková, K., Gentsch, N., Gittel, A., Guggenberger, G., Hugelius, G., Lashchinsky, N., Martikainen, P. J., Mikutta, R., Schlexer, C., Schneckner, J., Schwab, C., Shibistova, O., Wild, B., and Richter, A.: Significance of dark CO₂ fixation in arctic soils, *Soil Biol. Biochem.*, 119, 11–21, <https://doi.org/10.1016/j.soilbio.2017.12.021>, 2018.
- Sarathchandra, S. U., Perrott, K. W., and Littler, R. A.: Soil microbial biomass: Influence of simulated temperature changes on size, activity and nutrient-content, *Soil Biol. Biochem.*, 21, 987–993, [https://doi.org/10.1016/0038-0717\(89\)90034-5](https://doi.org/10.1016/0038-0717(89)90034-5), 1989.
- Schindlbacher, A., Rodler, A., Kuffner, M., Kitzler, B., Sessitsch, A., and Zechmeister-Boltenstern, S.: Experimental warming effects on the microbial community of a temperate mountain forest soil, *Soil Biol. Biochem.*, 43, 1417–1425, <https://doi.org/10.1016/j.soilbio.2011.03.005>, 2011.
- Schloss, P. D., Westcott, S. L., Ryabin, T., Hall, J. R., Hartmann, M., Hollister, E. B., Lesniewski, R. A., Oakley, B. B., Parks, D. H., Robinson, C. J., Sahl, J. W., Stres, B., Thallinger, G. G., Van Horn, D. J., and Weber, C. F.: Introducing mothur: open-source, platform-independent, community-supported software for describing and comparing microbial communities, *Appl. Environ. Microbiol.*, 75, 7537–7541, <https://doi.org/10.1128/AEM.01541-09>, 2009.
- Schnürer, J., Clarholm, M., Boström, S., and Rosswall, T.: Effects of moisture on soil microorganisms and nematodes: A field experiment, *Microb. Ecol.*, 12, 217–230, <https://doi.org/10.1007/BF02011206>, 1986.
- Schuur, E. A. G., McGuire, A. D., Schädel, C., Grosse, G., Harden, J. W., Hayes, D. J., Hugelius, G., Koven, C. D., Kuhry, P., Lawrence, D. M., Natali, S. M., Olefeldt, D., Romanovsky, V. E., Schaefer, K., Turetsky, M. R., Treat, C. C., and Vonk, J. E.: Cli-

- mate change and the permafrost carbon feedback, *Nature*, 520, 171–179, <https://doi.org/10.1038/nature14338>, 2015.
- Selesi, D., Schmid, M., and Hartmann, A.: Diversity of Green-Like and Red-Like Genes (cbbL) in Differently Managed Agricultural Soils, *Appl. Environ. Microb.*, 71, 175–184, <https://doi.org/10.1128/AEM.71.1.175-184.2005>, 2005.
- Six, J., Frey, S. D., Thiet, R. K., and Batten, K. M.: Bacterial and Fungal Contributions to Carbon Sequestration in Agroecosystems, *Soil Sci. Soc. Am. J.*, 70, 555–569, <https://doi.org/10.2136/sssaj2004.0347>, 2006.
- Soong, J. L., Phillips, C. L., Ledna, C., Koven, C. D., and Torn, M. S.: CMIP5 Models Predict Rapid and Deep Soil Warming Over the 21st Century, *J. Geophys. Res.-Biogeo.*, 125, e2019JG005266, <https://doi.org/10.1029/2019JG005266>, 2020.
- Soong, J. L., Castanha, C., Hicks Pries, C. E., Ofiti, N., Porras, R. C., Riley, W. J., Schmidt, M. W. I., and Torn, M. S.: Five years of whole-soil warming led to loss of subsoil carbon stocks and increased CO₂ efflux, *Science Advances*, 7, 1–9, <https://doi.org/10.1126/sciadv.abd1343>, 2021.
- Spohn, M., Klaus, K., Wanek, W., and Richter, A.: Microbial carbon use efficiency and biomass turnover times depending on soil depth – Implications for carbon cycling, *Soil Biol. Biochem.*, 96, 74–81, <https://doi.org/10.1016/j.soilbio.2016.01.016>, 2016.
- Spohn, M., Müller, K., Höschel, C., Mueller, C. W., and Marhan, S.: Dark microbial CO₂ fixation in temperate forest soils increases with CO₂ concentration, *Glob. Change Biol.*, 26, 1926–1935, <https://doi.org/10.1111/gcb.14937>, 2019.
- Stotzky, G. and Rem, L. T.: Influence of clay minerals on microorganisms. I. Montmorillonite and kaolinite on bacteria, *Can. J. Microbiol.*, 12, 547–563, 1966.
- Tsubo, M., Fukai, S., Basnayake, J., To, P. T., Bouman, B., and Harnpichitvitaya, D.: Effects of soil clay content on water balance and productivity in rainfed lowland rice ecosystem in Northeast Thailand, *Plant Prod. Sci.*, 10, 232–241, <https://doi.org/10.1626/pp.s.10.232>, 2007.
- Van 't Hoff, J. H.: Lectures on Theoretical and Physical Chemistry. Part 1. Chemical Dynamics, OCLC Number 220605730, Edward Arnold, London, 1898.
- Van Veen, J. A., Ladd, J. N., and Frissel, M. J.: Modelling C and N turnover through the microbial biomass in soil, *Plant Soil*, 76, 257–274, 1984.
- Van Veen, J. A., Ladd, J. N., and Amato, M.: Turnover of carbon and nitrogen through the microbial biomass in a sandy loam and a clay soil incubated with [¹⁴C(U)]glucose and [¹⁵N](NH₄)₂SO₄ under different moisture regimes, *Soil Biol. Biochem.*, 17, 747–756, [https://doi.org/10.1016/0038-0717\(85\)90128-2](https://doi.org/10.1016/0038-0717(85)90128-2), 1985.
- Vance, E. D., Brookes, P. C., and Jenkinson, D. S.: An extraction method for measuring soil microbial biomass C, *Soil Biol. Biochem.*, 19, 703–707, [https://doi.org/10.1016/0038-0717\(87\)90052-6](https://doi.org/10.1016/0038-0717(87)90052-6), 1987.
- Vijay, A., Chhabra, M., and Vincent, T.: Microbial community modulates electrochemical performance and denitrification rate in a biocathodic autotrophic and heterotrophic denitrifying microbial fuel cell, *Bioresource Technol.*, 272, 217–225, <https://doi.org/10.1016/j.biortech.2018.10.030>, 2019.
- Walker, T. W. N., Kaiser, C., Strasser, F., Herbold, C. W., Leblans, N. I. W., Woebken, D., Janssens, I. A., Sigurdsson, B. D., and Richter, A.: Microbial temperature sensitivity and biomass change explain soil carbon loss with warming, *Nat. Clim. Change*, 8, 885–889, <https://doi.org/10.1038/s41558-018-0259-x>, 2018.
- Way, D. A. and Oren, R.: Differential responses to changes in growth temperature between trees from different functional groups and biomes: a review and synthesis of data, *Tree Physiol.*, 30, 669–688, <https://doi.org/10.1093/treephys/tpq015>, 2010.
- Werner, R. A. and Brand, W. A.: Referencing strategies and techniques in stable isotope ratio analysis, *Rapid Commun. Mass Sp.*, 15, 501–519, <https://doi.org/10.1002/rcm.258>, 2001.
- Winkler, J. P., Cherry, R. S., and Schlesinger, W. H.: The Q₁₀ relationship of microbial respiration in a temperate forest soil, *Soil Biol. Biochem.*, 28, 1067–1072, [https://doi.org/10.1016/0038-0717\(96\)00076-4](https://doi.org/10.1016/0038-0717(96)00076-4), 1996.
- Wu, J., Joergensen, R. G., Pommerening, B., Chaussod, R., and Brookes, P. C.: Short Communication Measurement of Soil Microbial Biomass Automated Procedure, *Soil Biol. Biochem.*, 22, 1167–1169, 1990.
- Wu, X., Ge, T., Yuan, H., Li, B., Zhu, H., Zhou, P., Sui, F., O'Donnell, A. G., and Wu, J.: Changes in bacterial CO₂ fixation with depth in agricultural soils, *Appl. Microbiol. Biot.*, 98, 2309–2319, <https://doi.org/10.1007/s00253-013-5179-0>, 2014.
- Xiao, H., Li, Z., Chang, X., Deng, L., Nie, X., Liu, C., Liu, L., Jiang, J., Chen, J., and Wang, D.: Microbial CO₂ assimilation is not limited by the decrease in autotrophic bacterial abundance and diversity in eroded watershed, *Biol. Fert. Soils*, 54, 595–605, <https://doi.org/10.1007/s00374-018-1284-7>, 2018.
- Yin, H., Xiao, J., Li, Y., Chen, Z., Cheng, X., Zhao, C., and Liu, Q.: Warming effects on root morphological and physiological traits: The potential consequences on soil C dynamics as altered root exudation, *Agr. Forest Meteorol.*, 180, 287–296, <https://doi.org/10.1016/j.agrformet.2013.06.016>, 2013.
- Yuan, H., Ge, T., Chen, C., O'Donnell, A. G., and Wu, J.: Significant role for microbial autotrophy in the sequestration of soil carbon, *Appl. Environ. Microb.*, 78, 2328–2336, <https://doi.org/10.1128/AEM.06881-11>, 2012.